An experimental investigation into the whole body vibration generated during the hydroelastic slamming of a high speed craft

P. K. Halswell[1], P. A. Wilson[1], D. J. Taunton[1], and S. Austen[2]

[1] University of Southampton; [2] Royal National Lifeboat Institution.

Corresponding author: Dr P. K. Halswell, email address; peterhalswell@gmail.com, telephone; 07813390513, postal address; 12 Park Crescent, Falmouth, Cornwall, TR11 2DL.

Abstract

High-Speed planing Craft (HSC) expose their crew to levels of vibration that regularly exceed the daily exposure limit set out by European directive 2002/44/EU. The human exposure to vibration can cause many effects, from chronic and acute, to physiological and psychological. Many reduction methods are currently being researched, such as suspension seats, but Coats et al. (2003) and Coe et al. (2013) concluded that a combination of methods will be required to reduce the level sufficiently to meet the legislation. The highest levels of acceleration occur during the slamming of HSC.

This paper describes an experimental investigation to determine whether hydroelasticity can affect the slamming characteristics and Whole Body Vibration (WBV) of a HSC using quasi-2D and full-scale drop tests. The quasi-2D drop tests revealed that hydroelasticity can affect the peak acceleration and Vibration Dosage Value (VDV), and that a wooden hull generated higher magnitude WBV than fabric hulls. The full-scale drop tests were performed on a RNLI D-class inflatable lifeboat. Hydroelasticity was controlled using the internal pressures of the sponson and keel. The full-scale results show that the peak acceleration and VDV can be reduced by decreasing the internal pressures and structural stiffness at the transom and crew locations; however, this lead to an increase at the bow. This indicates that the WBV experienced by the crew can be reduced by considering hydroelasticity. Incorporating an element of hydroelasticity shows great potential, alongside other reduction strategies, to alleviate the human exposure to vibration on board HSC.

Keywords: Whole body vibration, mechanical shock, high speed crafts, rigid inflatable boats, inflatable boat, hydroelastic, slamming, drop tests.

Nomenclatures

c	Phase speed of wave (m/s)
cRIO	Compact reprogrammable input output
EAV	Exposure action value
ELV	Exposure limit value
fps	Frames per second
g	Acceleration due to Gravity (9.81 m/s^2)
h	Water depth (m)
HSC	High speed craft
NI	National Instruments
MDF	Medium density fibreboard
RIB	Rigid inflatable boat
RMS	Root mean square
RNLI	Royal National Lifeboat Institution
VDV	Vibration dosage value
WBV	Whole body vibration

1. Introduction

The Whole Body Vibration (WBV) generated by the boat motion of High Speed Craft (HSC) can cause many health risks because the crew are exposed to high magnitude accelerations. In 2002, the European directive 2002/44/EC was passed on the minimum health and safety requirements for the exposure of workers to physical vibration and was included in UK legislation since 2005, see Pond (2005) and MCA (2007). The European directive sets the Exposure Action Value (EAV) for Whole Body Vibration (WBV) at 0.5 ms^{-2} RMS (or 9.1 $ms^{-1.75}$ Vibration Dosage Value (VDV)) and the Exposure Limit Value (ELV) at 1.15 ms^{-2} RMS (or 21 $ms^{-1.75}$ VDV). VDV is used instead of Root Mean Square (RMS) when the crest factor is above six; crest factor is defined by peak acceleration divided by RMS acceleration. HSC in rough water exposes the crew to non-linear vibration that regularly exceed the EAV and ELV. The highest acceleration occurs during a slam and in the case of HSC this can involve the entire hull losing contact with the water surface. Ochi (1964) defined a slam when the relative motion exceeds the local effective draught and the relative velocity at impact, see Lloyd (1998) page 292. Dand (2004) experimentally tested a rigid scale-model of the Royal National Lifeboat Institution (RNLI) D-class inflatable lifeboat and measured accelerations of up to 4 g in the crew's position through regular waves;

full-scale wave height of 0.55 m and full-scale speed of 19.4 knots. Townsend et al. (2008) showed that the RNLI Atlantic 85 Rigid Inflatable Boat (RIB) exceeded the EAV in 30 minutes at 32 knots with approximately 0.4 m significant wave height. Allen et al. (2008) measured the vibrations on the RNLI Atlantic 75 in two trials at speeds of 15 knots to 20 knots. The crest factors were above 6; this meant VDV was used instead of RMS and the z-axis values were 48.51 $ms^{-1.75}$ and 25.90 $ms^{-1.75}$ in sea states two and three, respectively. Myers et al. (2011) measured the acceleration on board a military HSC at 40 knots in a sea state of two to three and the VDV for a 3 hour transit was 57.05 $ms^{-1.75}$ on the deck. This is clear evidence that the vibration within these craft regularly exceeds the ELV and a solution, or combination of solutions, must be found. Whilst there is considerable debate in the marine community over the validity of applying the European directive to HSC, the RNLI are investigating methods to demonstrably mitigate the exposure of their crews and trainers to vibration. The work is gratefully supported and funded by the RNLI and EPSRC.

The human exposure to vibration can have many effects; from chronic and acute, to physiological and psychological, see Townsend et al. (2012). Physiological injuries have been reported by Ensign et al. (2000) to include; spinal and abdominal injuries, damage to internal organs (kidneys), torn ligaments and, broken ankles and legs. Ensign et al. (2000) also reported that the psychological injuries include; annoyance, fatigue, anxiety, loss of visual accuracy and reduced hand-eye coordination (the latter two could be considered a combination of both physiological and psychological effects). Myers et al. (2011) demonstrated a three hour transit at 40 knot in HSC will reduce the physical performance of the crew (including run distance and vertical jump height). Therefore, reducing boat motion and human exposure to vibration can reduce the risk of injury, provide a better working environment and increase the crew's effectiveness during and after transit. Researchers have explored many technological solutions to this problem; however, no single solution appears to be completely successful. Coe et al. (2013) concluded that a combination of solutions will be required to reduce WBV sufficiently to meet legislation, which was also backed up by Coats et al. (2003). Suspension seats are currently been researched, see Coats et al. (2003); Cripps et al. (2004); Coe et al. (2009); Olausson (2012); Coe et al. (2013); although, Townsend et al. (2012) pointed out that there are many drawbacks. Townsend et al. suggested a number of other strategies to reduce the WBV: suspended decks (also discussed by Coe et al. (2013)), active and passive fins, trim tabs, interceptors, gyrostabilisers, flexible hulls and elastomer coated hulls. Coats et al. (2009) discussed the use of a porous hull to reduce impact

loads and spread the energy over a longer time period, and they showed a significant reduction in impact loads.

Figure 1: The RNLI B-class and D-class.

The RNLI D-class, see Figure 1, is a 5 m inflatable lifeboat capable of achieving 25 knots in sea states associated with Beaufort force 2 and can continue to operate safely up to and beyond sea states associated with Beaufort force 5. It is powered by a 50 horse-power tiller-steer outboard engine and weighs a total of 655 kg (including all equipment and three crew). It is operated by three crew and can rescue a minimum of two casualties or one in the prone position. The RNLI performed a feasibility study on the EA16 (the original version of the D-class) in 1998 and compared it to 7 commercially available vessels that included; RIBs, pure inflatable boats or a combination of both. It was found that the EA16 gave the best overall performance. Therefore, the RNLI have been improving its design and performance through either designers experience or trial and error to achieve the optimum boat. Anecdotal evidence from the feedback of the crew reported that flexibility within the D-class improves its performance, especially in waves and surf. The flexible interaction between the fluid and structure is defined using the term hydroelasticity, where the fluid applies a force to the structure which causes the structure to deform; simultaneously, the deformation of the structure causes a change in the fluid forces. There are four main structural components in the D-class, see Figure 2, which includes; inflatable sponson (also called collar or tube), segmented composite deck and transom, inflatable keel and fabric hull. Hydroelasticity of the D-class has been reviewed by Halswell et al. (2012) and provides readers with a good overview of the D-class.

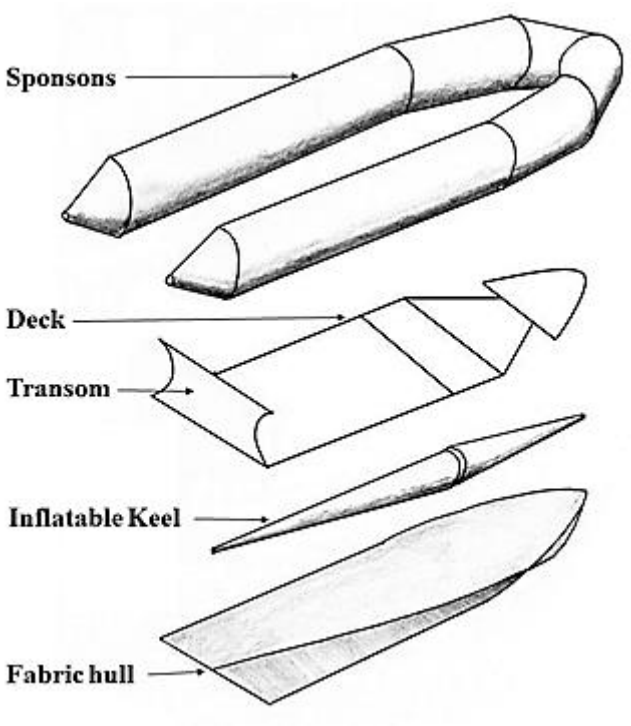

Figure 2: Main components of the D-class.

The first component in the D-class is the sponson and it has been proposed by Natzijl (1998) and Pike (2003) (and discussed by others in the maritime community) that the sponson is able to absorb energy during a slam but there is no scientific evidence. Haiping et al. (2005) experimental studied the effect of sponson type on sea keeping performance. It was found that an inflatable sponson had a lower response amplitude operator in heave and pitch than a foam sponson in two load conditions. This suggests that a flexible sponson can improve the ride quality and sea keeping. Townsend et al. (2008) performed experiments into sea keeping performance of the RNLI Atlantic 75 RIB and showed that the internal pressure of the sponson had minimal effect on sea keeping. They concluded that the sponson did not contact the water enough to affect sea keeping performance. So the D-class sponson could be responsible for the anecdotal evidence of improved performance because they are in full contact with the water during operation; however, there are three other flexible components (deck, keel and hull) that could also affect sea keeping and slamming characteristics. Townsend et al. (2012) numerically explored the effect of decreasing hull stiffness to isolate humans from vibration. The hull stiffness was reduced from 69 GPa to 6.9 GPa and found that it had little effect on the response. This suggests that hull stiffness has minimal effect on slamming characteristics; however, the rubber-coated fabric used for the D-class hull is more flexible than conventional hull materials. The D-class hull is constructed from two laminate sheets of Aerazar decitex 1100; a rubber coated fabric. Aerazar decitex 1100 is laminated

layers of neoprene, high tenacity textile (Polyester) and Hypalon®, see Figure 3. Aerazar decitex 1100 has a plain weave Polyester fibre, a woven weight of 250 g/m^2, gauge of 0.85 mm, and gauge weight of 980 g/m^2. Table 1 compares the properties of Aerazar decitex 1100 (weft; transverse direction on the hull) to the properties of aluminium. First, the Young's modulus of the fabric is nearly 250 times lower than aluminium and 25 times lower than the work of Townsend et al. (2012). Next, the density of the fabric is 57% less than aluminium; although, the ultimate tensile strength is only 27% lower. The static central deflection of a 1 m square plate to a 1000 N central point load was predicted to quantify deflection difference between a typical aluminium hull and a fabric hull under comparable conditions. The deflection of a fabric hull is 4.4 times greater than an aluminium hull. Therefore, it is anticipated that this degree of elasticity will affect slamming characteristics.

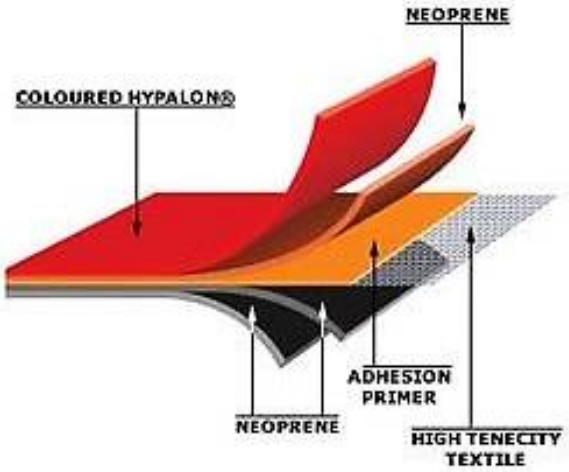

Figure 3: Construction of rubber coated-fabric, Hot RIBS (2015).

Table 1: Fabric properties vs. aluminium properties.

Property	Hull fabric (weft)	Aluminium
Young's modulus (GPa)	0.28	69
Ultimate tensile strength (MPa)	> 80	110
Density (kg/m^3)	1152	2700
Static deflection of square 1m plate to 1000 N central point load (mm)	41.6[1]	9.4[2]

[1] Predicted using Equation 1 of Maier-Schneider et al. (1995), where: p = 1000 N/m^2, C_1 = 3.04, C_2 = 1.83, a = 0.5 m, t = 1.7 mm, E = 0.28 GPa, σ = 0 N/m^2 and ν = 0.3.

[2] Predicted using SolidWorks 2014 static simulator with large deflection, where: length = 1000 mm, width = 1000 mm, thickness = 2.5 mm, material = Aluminium 1060 (E = 69 GPa, ν = 0.33), full constrained edge boundaries conditions and 1000 N load applied to 10 mm diameter central point. Hull thickness of 2.5 mm used by Ribeye TS/TL series, see http://www.ribeye.co.uk/the-build assessed 14/11/2015.

The structure of the D-class is able to deform more than a conventional planing craft. The longitudinal deformation of the D-class is observable during static loading, drop tests and wave trials (as seen by the author) but this deformation is not observable for conventional planing craft. Furthermore, the static hull panel deflection on the D-class approximately four times greater than equivalent conventional planing craft, see Table 1. The hydroelastic interaction caused by the D-class deformation may change the slamming characteristics. Slamming characteristics can be defined as either: magnitude and duration of peak acceleration or integration of acceleration-time history (VDV). The slamming characteristics indicate the severity of human exposure to vibration; therefore, is it possible to use hydroelasticity to reduce the human exposure to vibration? Drop tests have been utilised to investigate the effect of structural stiffness (and hydroelasticity) on the slamming characteristics; both model-scale quasi-2D and full-scale D-class drop tests. The aims can be summarised as:

1. Measure the effects of pre-tensioned stress in a fabric hull on the slamming characteristics of a planing vessel using quasi-2D drop tests.
2. Measure the effects of internal pressures in the sponson and keel of the RNLI D-class on the slamming characteristics during full-scale drop tests.
3. Quantify the change in human exposure to vibration by changing the structural stiffness of a planing vessel.

2. Experimental Methods

2.1. Quasi-2D Drop Tests

It is hypothesised that the pre-tensioned stress in the fabric hull of the RNLI D-class will affect the slamming characteristics.

2.1.1 Equipment

The quasi-2D drop test rig is shown in Figure 4 and is the same rig used by Lewis et al. (2010). A pulley system adjusted the drop height. The wedge ran along two vertical poles via four bearings to ensure a vertical impact, released using a quick release shackle. The accelerometer screwed to the steel frame of the wedge. The wedge was designed to test composite panels at a variable deadrise angle (5°, 15° and 25°) but a special fabric panel was wrapped around the wedge to form a fabric hull. The fabric was constructed from two laminated sheets of Aerazar decitex 1100 rubber-coated fabric; same material and lay up found on the D-class hull. A turn-buckle mechanism adjusted the pre-tension stress in the

fabric hull. The wedge dropped into a water tank; 5.8 m long, 0.75 m wide and 0.5 m water depth. There was an observation window (0.825 m × 0.485 m) in the centre of the tank.

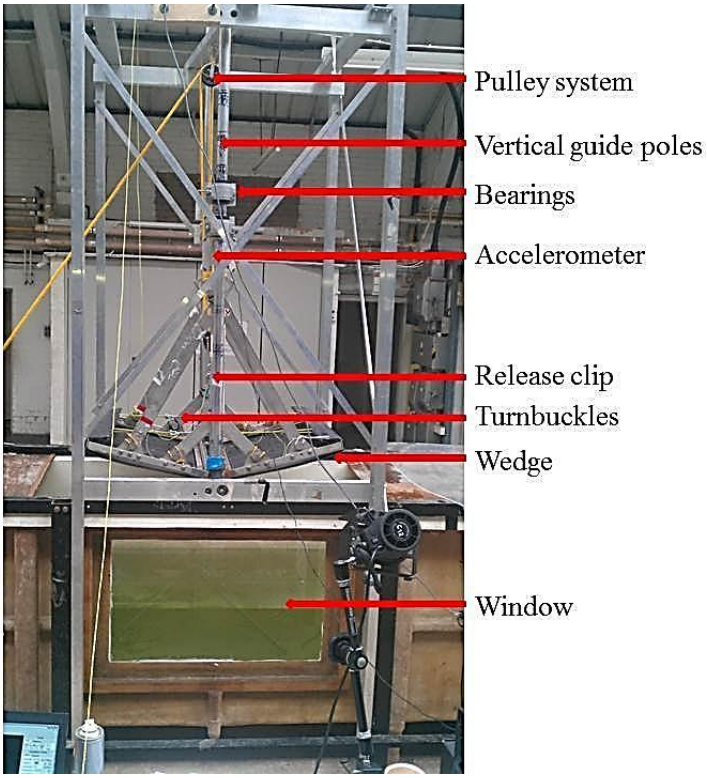

Figure 4: Quasi-2D drop test rig.

A Crossbow CXL-HF accelerometer measured the acceleration with a sensitivity of ±10 mV/g and a range of ±100 g; it was not DC-coupled so could not measure free fall. A DaqLab 2000 series data acquisition system logged the data with a sampling frequency of 5000 Hz and an accuracy of ±0.1 mV. The combined system gave a predicted accuracy of ±0.01 g. A Redlake MotionPro X high-speed monochrome camera recorded the event at 2000 frames per second (fps).

2.1.2 Parameters

The main parameters affecting the slamming characteristics of quasi-2D drop tests are deadrise angle, drop height and mass. The paper does not intend to scale the quasi-2D test to full-scale because "the methods to extrapolate the results of model to full scale are not yet developed", see Kapsenberg (2011). The deadrise angle of the D-class varies from 0° at the transom to a maximum of 15°; therefore, the variable deadrise angle wedge was tested at 5° and 15°. A 0° deadrise angle was not tested because other phenomena (such as air cushioning) occur at deadrise angles below 4°, see Bereznitski (2001). The drop heights of 0.5 m and 1 m were tested, which corresponds to impact velocities of 3.13 m/s and 4.43 m/s,

respectively. . The mass of the wedge was 50.2 kg. The transverse width of the wedge, diagonally from keel to chine, was 0.501 m and the horizontal width (chine to chine) is 0.998 m and 0.968 m at deadrise angles of 5° and 15°, respectively.

The main variable of the quasi-2D drop tests was hull stiffness and three stiffness conditions were chosen; fabric hull with 0 N/m and 1000 N/m of pre-tensioned stress and wooden hull. The wooden hull condition was represented by a 6 mm sheet of Medium Density Fibreboard (MDF) (6 mm thickness was the correct panel thickness for the wedge) and the Young's modulus of MDF was approximately 4 GPa. MDF was chosen for its light weight and isotropic material properties. The static central deflection of a 1 m MDF square plate (6 mm thickness) to a 1000 N central point load predicted using SolidWorks, same method as Table 1, was 17.5 mm; therefore, the fabric hull under 0 N/m pre-tensioned stress was approximately 2.4 times greater than the wooden hull under the preceding static conditions. Lewis (2003) stated that varying the pre-tensioned stress within a fabric will have the same effect as varying the material properties, so only pre-tensioned stress was varied. The real pre-tensioned stress in the D-class hull is unknown but, in places, the tension is very low because the fabric is very loose; therefore, one stiffness condition was used to represent zero hull tension (0 N/m). It was unclear how much more tension would result in a measurable difference so 1000 N/m was used. The pre-tensioned stresses were only applied in the transverse direction and were measured using strain. The non-linear material properties of hull fabric showed that a tension of 1000 N/m produced a strain of 0.005. The boundary conditions of the fabric hull were pin joints along the chine and centreline, see Figure 5a, but were effectively roller joints along the two transverse edges, only restricting the out-of-plane deflection, see Figure 5b. The boundary conditions of the MDF hull were fully clamped along all edges, see Figure 5c.

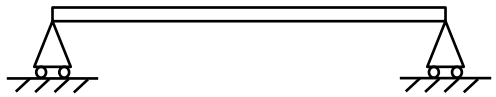

(a) Longitudinal view of fabric hull.

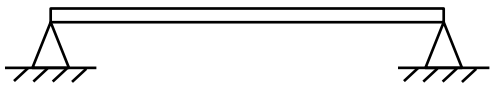

(b) Transverse view of fabric hull.

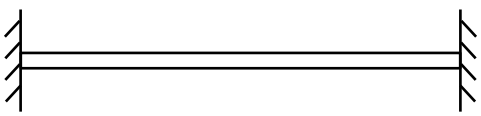

(c) Longitudinal and transverse view of wooden hull.

Figure 5: Boundary condition of quasi-2D drop test hulls.

2.1.3 Procedure

1. The deadrise angle and pre-tensioned stress were set.
2. The wedge was raised to the desired drop height.
3. The water was allowed to settle so that the surface movement was less than ±5 mm.
4. The data acquisition system and high speed camera were started.
5. The wedge was released.
6. The data acquisition system and high speed camera were stopped.
7. The procedure was repeated from step two to acquire three repetitions.

2.1.4 Post processing

Post processing of the acceleration time signal was required to: synchronising and cropped time history, apply W_b frequency weighting, calculate VDV and transformation into frequency spectrum. All post processing was performed in MatLab. The quasi-2D drop test acceleration signals were synchronised using a threshold of greater than 9.81 m/s^2 (because the accelerometer was not DC coupled so a 0 m/s^2 threshold was not appropriate), then cropped from theoretical free fall time (i.e. 0.316 s and 0.447 s for 0.5 m and 1 m drop height, respectively) before the threshold and one second after the threshold. The W_b frequency weighting was applied using the Human Vibration (HV) Lab toolbox of MatLab. VDV was calculated using Equation 1. The frequency spectrum was calculated using a second order Fast Fourier Transformation (FFT) function of MatLab.

Equation 1: VDV formula.

$$VDV = \left(\int_0^T a^4(t) dt \right)^{1/4}$$

2.2 Full-Scale Drop Tests

It has been hypothesised that the internal pressures in the sponson and keel will affect the slamming characteristics of the RNLI D-class.

2.2.1 Equipment

The experimental set up of the full-scale drop tests can be seen in Figure 6. The D-class was lifted with a crane and a drop height gauge (a marked length of rope) was fitted to the transom to measure the drop height. The drop height gauge had an accuracy of ±10 mm. A slip hook was used as a quick release mechanism which could be activated from the shore.

The bungee cord was required to stop the heavy shackles (used for trim angle adjustment) from impacting the deck and causing unwanted structural vibration. The trim angle was adjusted using various boat harnesses of different lengths. A GoPro Hero 2 recorded the drops at 120 fps. Finally a remote trigger was used to start the data acquisition system.

Three CFX USCA-TX tri-axial accelerometers measured the accelerations with an accuracy of ±0.2 V/g and were screwed to the deck panels. They had a range of ±20 g with a DC to 200 Hz flat frequency response; above 200 Hz the accelerometers had a -6 dB response. The accelerometer signals were wired into a National Instruments (NI) 9234 C-series accelerometer module. The module had an input range of ±5 V, a 24 bit analogue to digital converter, a built in anti-aliasing filter and an accuracy of ± 50 ppm. This combined system has a predicted accuracy of ±250 μg. The locations of the accelerometers are shown in Figure 7. The first accelerometer was fitted to the transom next to the helm and the second accelerometer was fitted to the deck between the knees of the crew. These accelerometers measured the vibration of the structure at the point of contact between the helm or crew to provide an estimation of the accelerations experienced by the helm or crew. The final accelerometer was fitted near the bow to investigate how the vibration changes along the length of the D-class. The data logger was a NI 9074 compact Reprogrammable Input Output (cRIO) device. The cRIO was inside a waterproof case with its own battery to form a standalone data acquisition system, which was then strapped to the deck. The cRIO saved the data to two SD cards through a NI 9802 C-series SD card module at a sampling frequency of 2500 Hz.

2.2.2 Parameters

The main parameter for the full-scale drop test was the internal pressures of the sponson and keel. Three internal pressure conditions were chosen, the standard operating pressures and ±1 psi. The standard operating pressures are 3.25 psi in the sponson and 3 psi in the keel; therefore, the three internal pressure conditions were 2.25 psi and 2 psi, 3.25 psi and 3 psi, and 4.25 and 4 psi in the sponson and keel, respectively. The internal pressures of both the sponson and keel are referred to as 2 psi, 3 psi and 4 psi for simplicity where in reality the internal pressure of the sponson was 0.25 psi higher. It was difficult to judge how much variation would be required to have a distinct effect on the slamming characteristics but anecdotal evidence from experienced helmsmen showed that a 0.25 psi change in the keel pressure would change the performance. This suggested that a variation of ±1 psi would affect the overall response of the boat. The drop heights of the full-scale drop tests matched

the drop heights used in the quasi-2D drop tests; 0.5 m and 1 m. The boat was always released at the same trim angle of 4.25° and this was as close to the running trim angle that could be achieved with the various boat harnesses. Dand et al. (2008) measured a running trim angle of four degrees. The trim angle was measured with a calibrated spirit level that had an accuracy of ±0.25°.

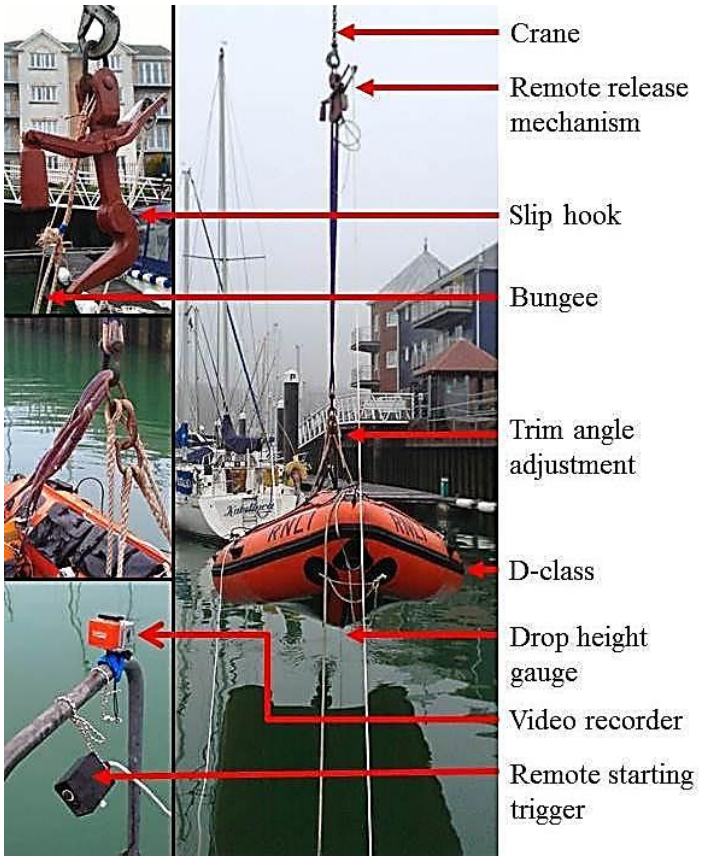

Figure 6: Full scale drop test set-up.

2.2.3 Procedure

1. The internal pressures were set.
2. The boat was raised to the desired drop height.
3. The boat and water surface was allowed time to settle so that the surface variation was less than ±10 mm (measured using the drop height gauge).
4. The data acquisition system and video recorder were started.
5. The D-class was released.
6. The data acquisition system and video recorder were stopped.
7. The procedure was repeated from step two to six for five repetitions.

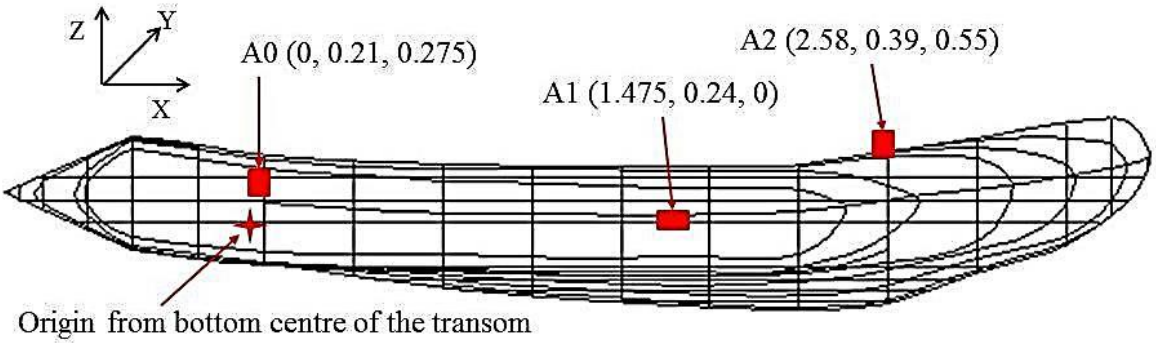

Figure 7: Location of accelerometers during the full-scale drop tests (m).

2.2.4 Post Processing

Post processing of acceleration time signal from the full-scale tests was the same as the quasi-2D tests (discussed in Section 2.1.4), except the threshold was 0 m/s^2 because the accelerometers were DC coupled and able to measure free fall.

2.3 Quantifying Whole Body Vibration

The quasi-2D and full-scale drop tests measure mechanical shock generated during a slam and not WBV; therefore, the first step in quantifying the effect of hydroelasticity on WBV is to relate mechanical shock to WBV. First of all, the acceleration signals must be frequency weighted to account for the frequency dependent response of the human body. The European directive 2002/44/EC recommends using ISO 5349-1:2001 W_b frequency weighting, shown in Figure 8. The W_b frequency weighting shows the human body has the largest dynamic response to frequencies between 2 Hz and 20 Hz. Furthermore, the W_b frequency weighting attenuates frequencies less than 0.1 Hz or greater than 100 Hz. The W_b frequency weighting has been applied herein, see Section 2.1.4; this is the most important step to relate mechanical shock to WBV.

Drop tests are under-damped sinusoidal systems that can be characterised using conventional parameters, such as: peak acceleration, peak duration and damping ratio. Peak acceleration and peak duration are clear and true indicators of the acceleration magnitude on the human body after applying the W_b frequency weighting. Furthermore, peak acceleration can be compared to the peak counting method for assessing the WBV from HSC with forward speed, such as Allen et al. (2008) and Myers et al. (2011). Peak counting can be compared to peak acceleration because a reduction in peak acceleration would indicate that the peak counting magnitudes would also reduce; however, the non-linear response of a HSC is not considered. Furthermore, the peak acceleration is proportional to the peak load

experienced by the crew via Newton's second law of motion (F = ma). The peak load can be compared to the load amplitude used by Schmidt et al. (2012). The comparisons to peak counting and load amplitude provide justification for using peak acceleration as a primary performance indicator.

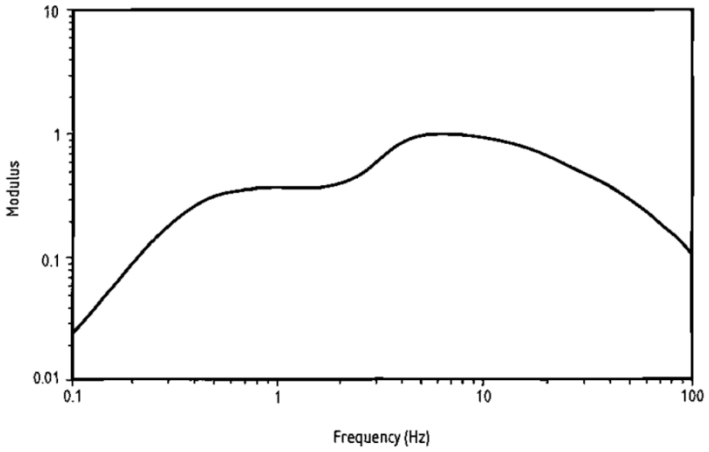

Figure 8: W_b frequency weighting, see BS 6472-1:2008.

The primary method to evaluate WBV is the RMS of the acceleration signal; however, the RMS is highly dependent on the time period and the peak acceleration is averaged out. The European directive states that if the crest factor is above six then the VDV should be used instead. The VDV was not formulated for an individual mechanical shock but it is best practice and provides another evaluation method. To the authors' knowledge there are no standards for evaluating the effect of individual mechanical shocks on a human. The crew of the D-class kneel in the boat and there is no frequency weighting for a kneeling position; only seated or standing position. It is anticipated that a frequency weighting for kneeling would be between seated and standing because the knees and hips are still able to rotate but not the ankles. The standing VDV is 0.4 of the seated VDV. Only the seated VDV will be reported as the standing VDV will follow the same trends. The seated VDV provides an over estimation assuming the keeling frequency weighting is between seated and standing frequency weighting.

3 Results

3.1 Quasi-2D Drop Tests

3.1.1 Accelerations

The time domain acceleration signals from the quasi-2D drop tests were first transformed into the frequency domain, using a second order FFT, to check for sources of noise. The mean frequency spectra, unfiltered and W_b frequency weighted, are shown in

Figure 9 for the drop tests at 5° deadrise angle, 1 m drop height and 1000 N/m fabric pre-tension. The frequency spectra are very similar to the spectra in reported Lewis et al. (2010), who used the same test rig. Lewis et al. used a 250 Hz low pass filter to remove the unwanted frequencies around 600 Hz; however, the W_b frequency weighting used here also removed the unwanted frequencies. The origin of the 600 Hz peak is unknown. The W_b frequency weighting reduced the power of frequencies below 4 Hz or above 10 Hz but amplified the power of frequencies between 4 Hz and 10 Hz. Frequencies above 30 Hz (and below 500 Hz) were negligible; less than one percentage of maximum power.

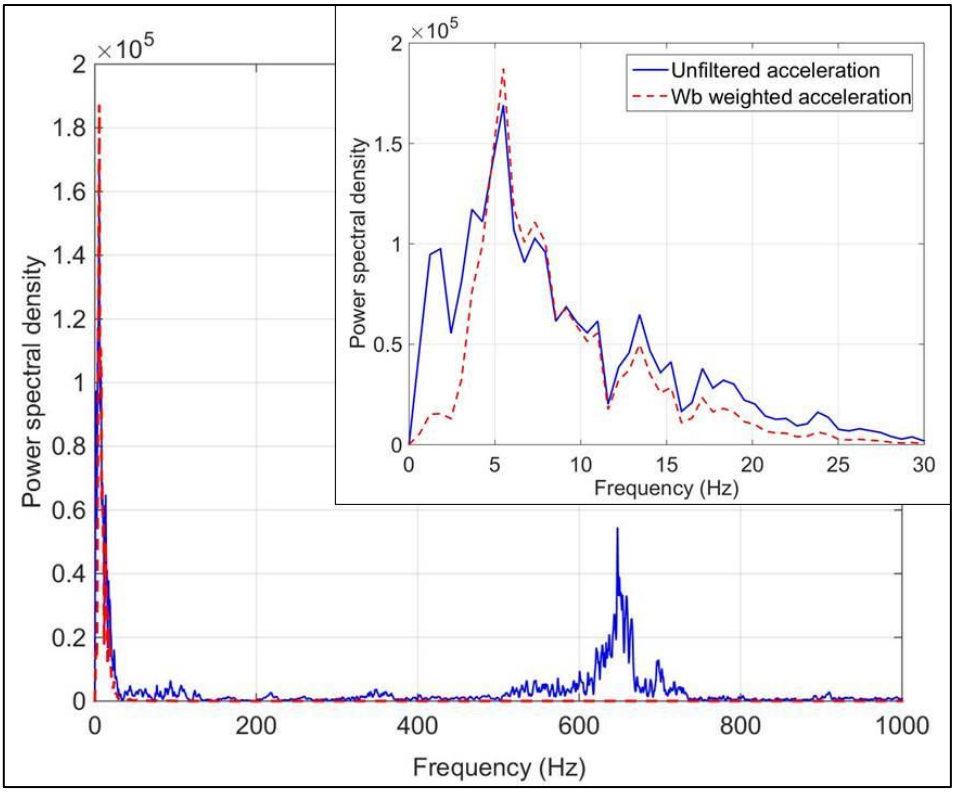

Figure 9: Mean frequency spectrum of the quasi-2D drop tests at 5° deadrise angle, 1 m drop height and 1000 N/m pre-tension.

The effect of the W_b frequency weighting on the mean acceleration-time history is shown in Figure 10 for the drop tests at 5° deadrise angle, 1 m drop height and 1000 N/m fabric pre-tension. First, the majority of the free fall stage was removed due to the 2 Hz high pass filter within the W_b frequency weighting. Second, the main peak amplitude at 0.5 s was reduced by approximately 50% but the main negative peak amplitude at 0.55 s was increased. Finally, there was minimal change to the free vibration stage after 0.8 s.

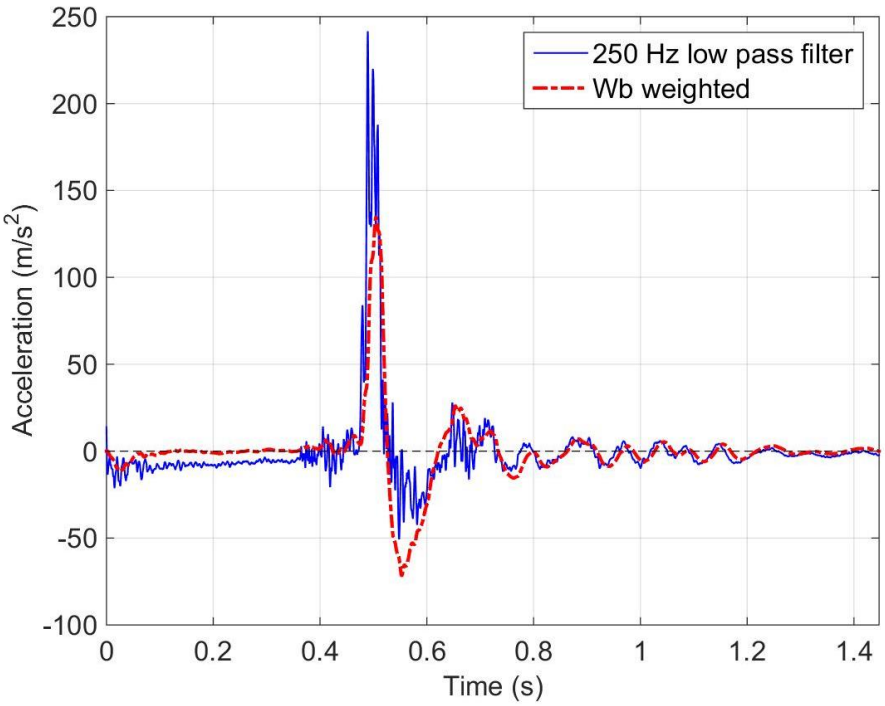

Figure 10: Mean acceleration-time history of the quasi-2D drop tests at 5° deadrise angle, 1 m drop height and 1000 N/m pre-tension.

The mean acceleration-time histories from three stiffness conditions (MDF, 1000 N/m and 0 N/m) at two deadrise angles and two drop heights can be seen in Figure 11 and Figure 12. The free fall stage, the first stage of acceleration-time histories, exhibited noticeable differences between the 0.5 m and 1 m drop heights; caused by wedge impacting the edge of the water tank. At 1 m drop height, the wedge built up momentum before impacting the tank so the impact had minimal effect on the acceleration but, at 0.5 m drop height, the lack of momentum caused a noticeable effect on the acceleration of the free falling wedge. However, the effect was repeatable throughout the drop tests.

The main positive and negative peaks, the second stage, did vary from changing the stiffness condition but the variation was more distinct at 5° deadrise angle. The most noticeable effect of the hull stiffness condition was at 1 m drop height and 5° deadrise angle, see Figure 12b. The MDF hull peaked at 170.8 m/s^2 but the fabric hull with 1000 N/m pre-tension only peaked at 134.6 m/s^2 (26.9% increase in peak acceleration). Importantly, the MDF hull did experience larger positive and negative peak accelerations than the fabric hulls under all conditions, except 15° deadrise angle and 0.5 m drop height. Furthermore, there was a difference in peak duration between the fabric and MDF stiffness conditions; again more distinct at 5° deadrise angle. The duration of the MDF hull peak acceleration was shorter than the duration of the fabric hull peak acceleration.

The free vibration stage, the third stage, did noticeably change between each stiffness condition, drop height and deadrise angle. The dynamic response of MDF hull was similar to a regular under-damped sinusoidal system, except the second peak was smaller than the third peak; however, the response of the fabric hulls did not represent a regular sinusoidal system. This shows that the damping ratio and degrees of freedom have changed between the MDF and fabric hulls. The damping ratios were generally larger in the fabric hulls.

3.1.2 Deformations

High speed images of the impact through the side observation window are shown in Figure 13. The wedge is moving down the image and the fabric can be seen wrapped around the wedge. The drop test condition was 15° deadrise angle, 1 m drop height and 0 N/m pre-tension. The first image shows the moment of impact. The second image shows that the fabric behind the wetted edge was pulled taught and ahead of the wetted edge the fabric was deformed. The third image shows that the fabric deformation moved with the wetted edge and continued until the wetted edge was outside the viewing window. The forth image shows an interesting observation that occurs near the end of an impact, which was a set of ripples in the fabric. This could have been caused by high out-of-plane forces in the centre of the panel or a reflected structural vibration. Three ripples were observed in a preparatory test when the fabric tension was very loose and occasionally the ripples were unnoticeable under higher pre-tensioned conditions.

3.1.3 Error Analysis

The boundary conditions between the MDF and fabric hull were slightly different; where the fabric hull was a pin joint and the MDF hull was fully clamped. This will affect the panel deflection but the fully clamped boundary conditions of the MDF hull will reduce the panel deflection because rotational deflection is constrained, see Figure 5. This means the MDF hull can be considered stiffer that the fabric hull. Furthermore, a fabric is defined because it has no out-of-plane bending stiffness; therefore, a fully clamped boundary condition will not remove rotational deflection of a fabric. So this change in boundary condition should not affect the response of the fabric.

When the wedge impacted the free surface it generated a wave, which was reflected off the end walls of the tank and might interfere with the impact and measured accelerations. The speed of shallow water waves can be calculated using $c^2 = gh$; where c is wave celerity, g is gravity (9.81 m/s^2) and h is water depth (0.5 m). The wave celerity was 2.214 m/s. The

tank was 5.8 m wide so the wave would take 2.62 s to reflect and collide with the impacting wedge. This shows that the reflected wave did not affect the measured accelerations.

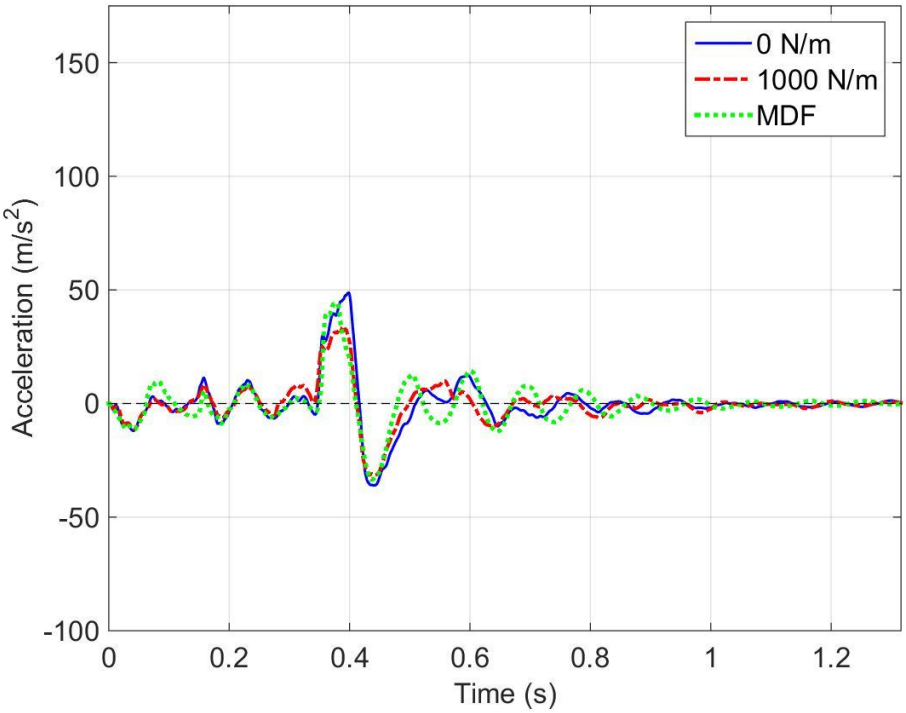

(a) 0.5 m drop height.

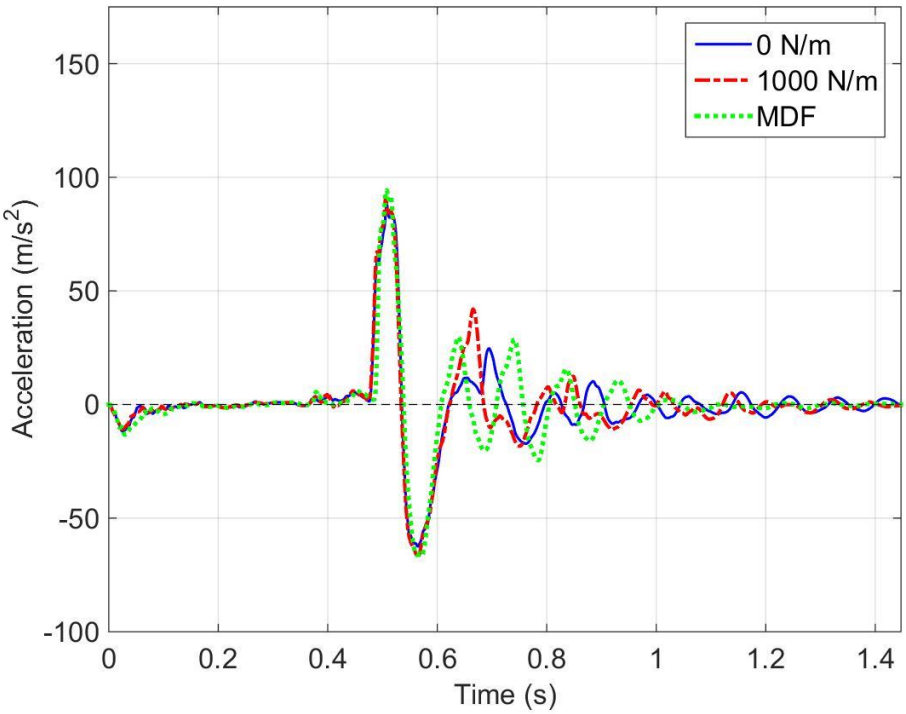

(b) 1m drop height.

Figure 11: Mean acceleration-time history (W_b weighted) from the quasi-2D drop test at 15° deadrise angle.

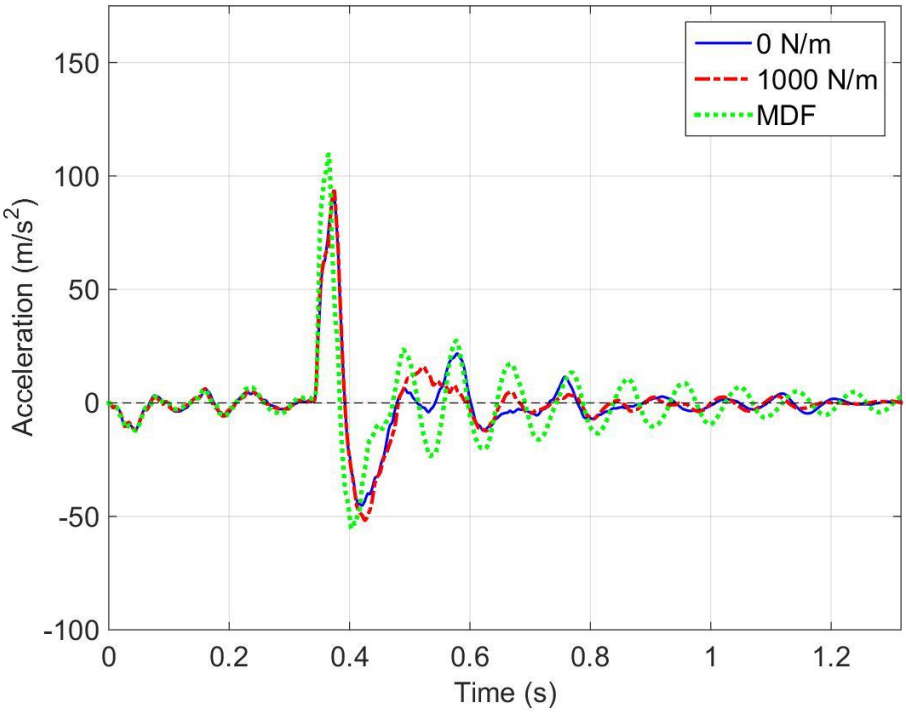

(a) 0.5 m drop height.

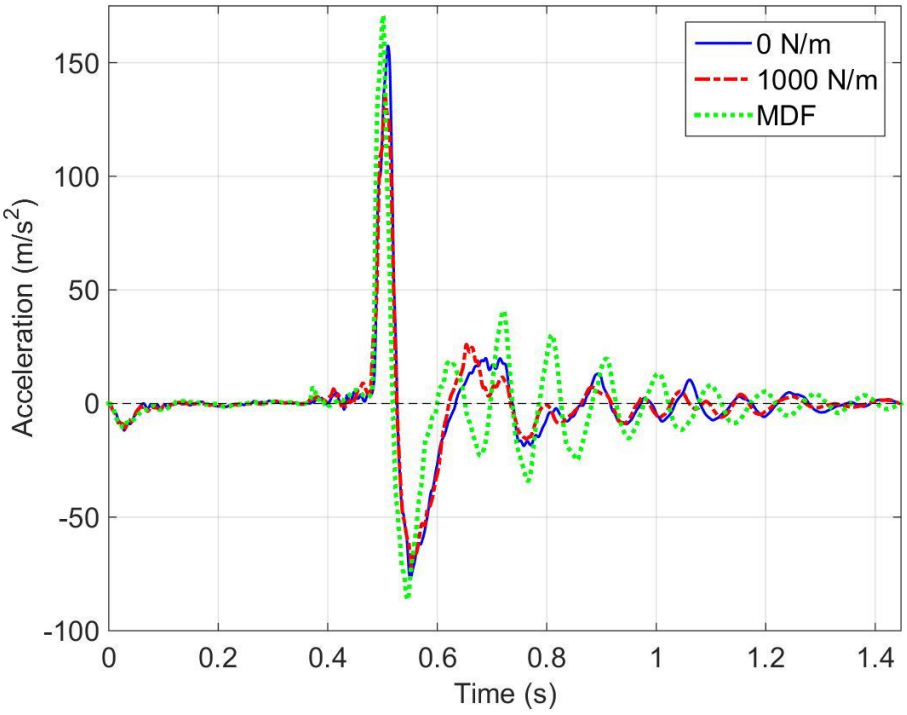

(b) 1m drop height.

Figure 12: Mean acceleration-time history (W_b weighted) from the quasi-2D drop test at 5° deadrise angle.

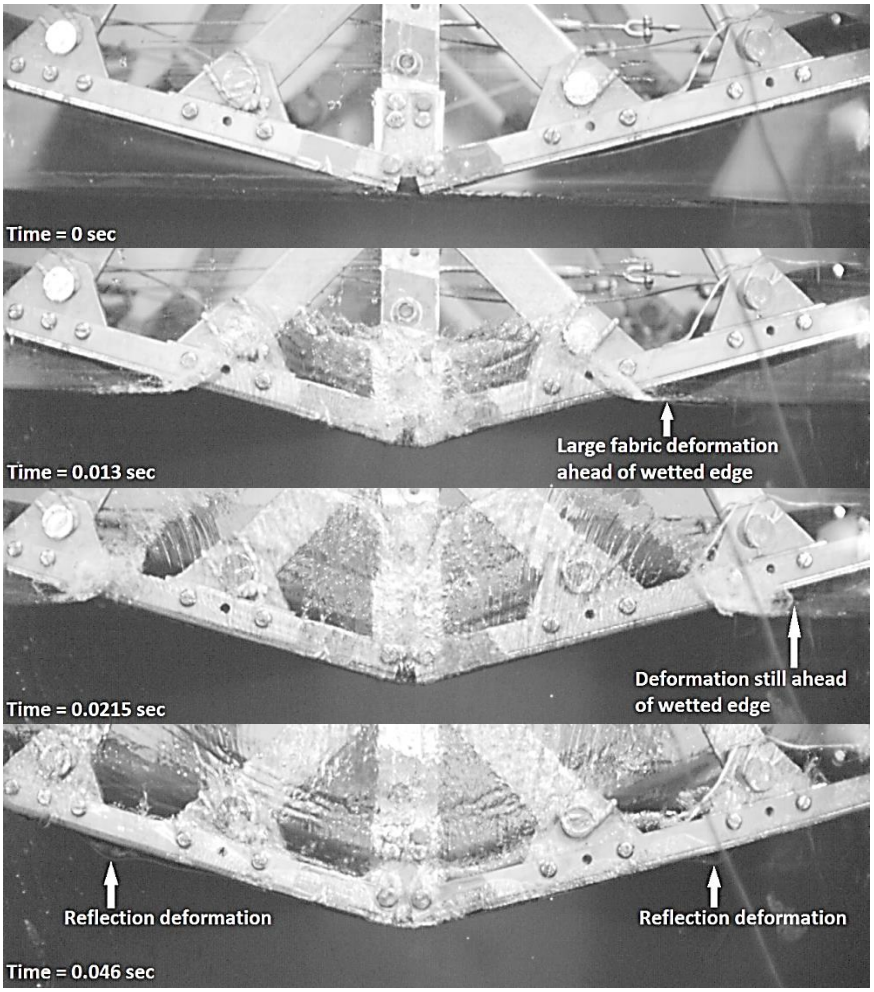

Figure 13: Transverse images of 2D drop test with a fabric hull under 0 N/m (15 degrees deadrise angle, 1 m drop height).

3.2 Full-Scale Drop Tests

3.2.1 Accelerations

A second order FFT was employed to transform the time domain acceleration signal from the full-scale drop tests into the frequency domain to check for unwanted sources of noise. The mean frequency spectra, unfiltered and W_b frequency weighted, from the crew accelerometer at 0.5 m drop height and 3 psi internal pressure are shown in Figure 14. The majority of the power in the frequency spectra was between 1 and 20 Hz with minimal above 20 Hz. No frequencies were noticeable (< 1% of peak power) in the unfiltered frequency spectrum above 200 Hz, due to the -6 dB above 200 Hz frequency response of the acceleration. The frequency spectra also show the effect of W_b frequency weighting. The weighting has significantly reduced frequencies below 4 Hz, amplified frequencies between 5 Hz and 7.5 Hz and a minor reduction in frequencies above 10 Hz.

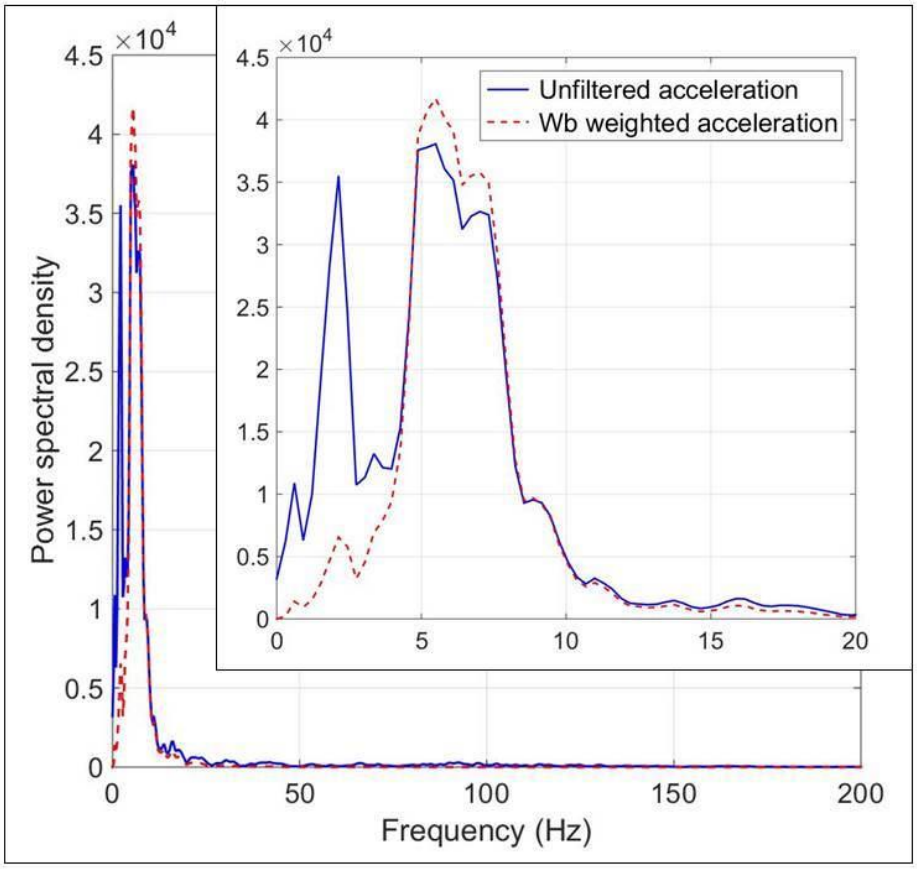

Figure 14: Mean frequency spectra from crew acceleration at 0.5 m drop height and 3 psi internal pressure.

The effect of W_b frequency weighting on the acceleration-time history is shown in Figure 15 for the full-scale drop tests at 0.5 m drop height and 3 psi internal pressure. The effect of W_b frequency weighting on the full-scale tests are similar to that of the quasi-2D tests. The free fall stage was removed and the positive peak acceleration was reduced; however, the negative peak was amplified in some instances and attenuated in others. The boat motion can also be seen in Figure 15 from the synchronised helm, crew and bow accelerometers. First, the transom impacted the water surface because it was dropped at 4.25° trim angle and the helm accelerometer experienced a large positive acceleration. Next, the crew accelerometer experienced a large positive acceleration 0.1 s after the helm accelerometer, followed shortly by the bow accelerometer.

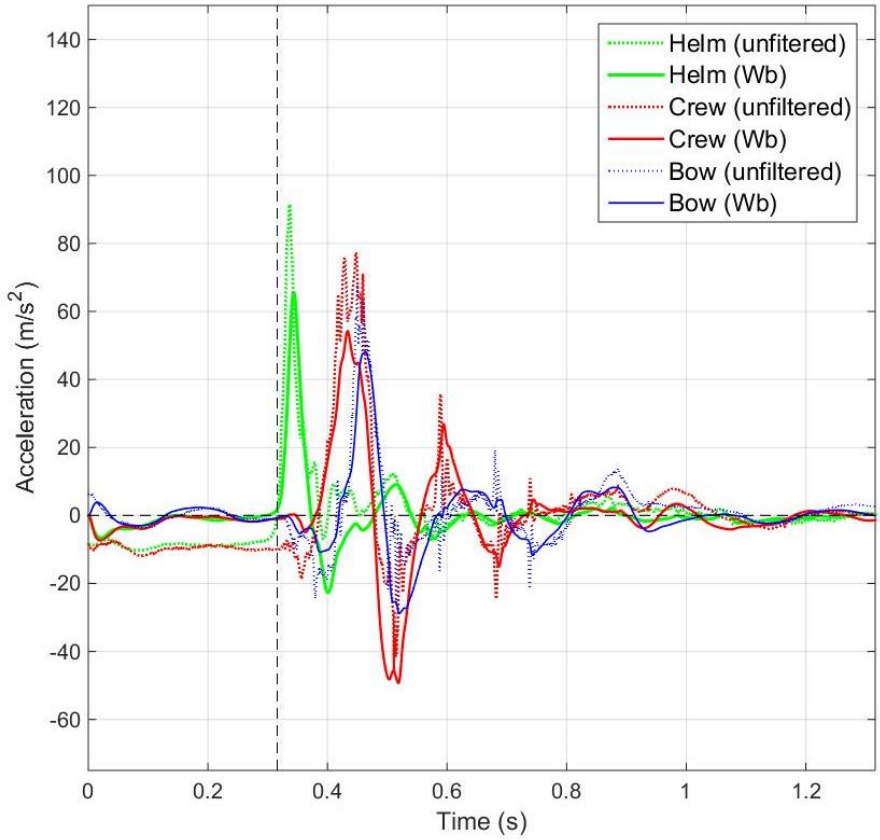

(a) 0.5 m drop hieght.

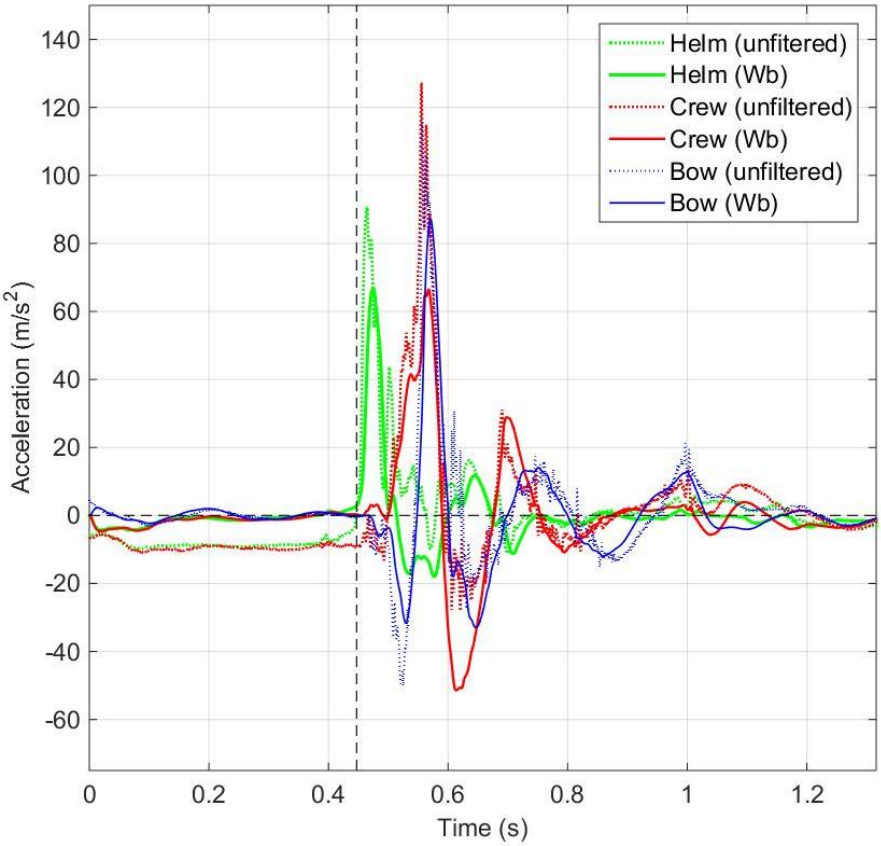

(b) 1 m drop hieght.

Figure 15: Mean acceleration-time history from each accelerometer during the full-scale drop tests at 0.5 m drop height and 3 psi internal pressure to show effect of W_b weighting.

The acceleration-time histories of the full-scale drop tests from helm, crew and bow accelerometers are shown in Figure 16 to Figure 18. All acceleration-time histories first show a repeatable free fall stage of 0 m/s^2 (due to W_b frequency weighting), then the major positive peak acceleration followed by a negative peak acceleration and, finally, a heavily damped free vibration stage. The overall impacts did follow an under-damped sinusoidal system but there were irregularities causing an inconsistent damping ratio. The damping was lower than observed in real seas with forward speed, for example Riley et al. (2010).

The internal pressures of the sponson and keel had minimal effect on accelerations measured by the helm acceleration. There was a slight difference in the peak accelerations but a more noticeable effect on the damping in the free vibration stage. The effect of internal pressure was greater in the crew and bow accelerometers than the helm accelerometer; however, this was expected because the structure at the transom is considerably stiffer than the rest of the boat. The inflatable keel does not extend right up to the transom, which removes the effect of the keel pressure all together. The vertical transom panel will dramatically reduce sponson rotation and this should reduce the effect of the sponson pressure. At 0.5 m drop height, the crew accelerometer measured a reduction in peak acceleration from 58 m/s^2 at 4 psi internal pressure to 43 m/s^2 at 2 psi internal pressure. Furthermore, the peak acceleration measured by the crew accelerometer reduced from 79 m/s^2 at 4 psi internal pressure to 55 m/s^2 at 2 psi internal pressure with 1 m drop height. On the other hand, the bow accelerometer measured an increase in peak acceleration from 42 m/s^2 at 4 psi internal pressure to 65 m/s^2 at 2 psi internal pressure with 0.5 m drop height. Additional, the bow accelerometer also measured an increase in peak acceleration from 96 m/s^2 at 4 psi to 110 m/s^2 at 2 psi with 1 m drop height. Therefore, the peak acceleration measured by the crew accelerometer has been reduced by reducing the internal pressures of the sponson and keel; however, peak acceleration measured by the bow accelerometer has been increased as a consequence.

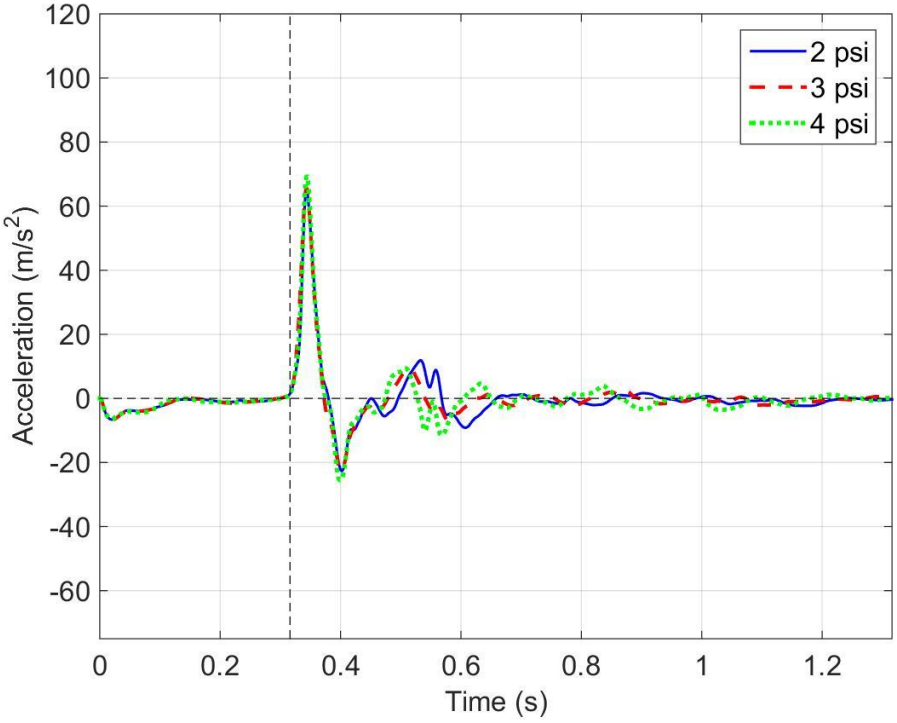

(a) 0.5 m drop hieght.

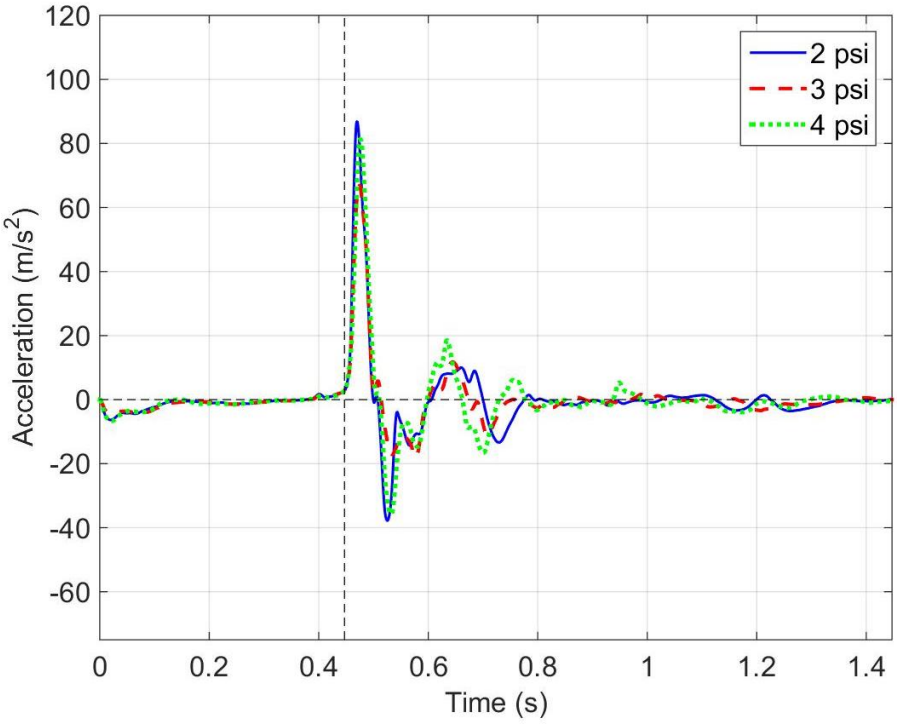

(b) 1 m drop hieght.

Figure 16: Mean acceleration-time history from the transom accelerometer (W_b weighted) during the full-scale drop tests with varied internal pressure of sponson and keel.

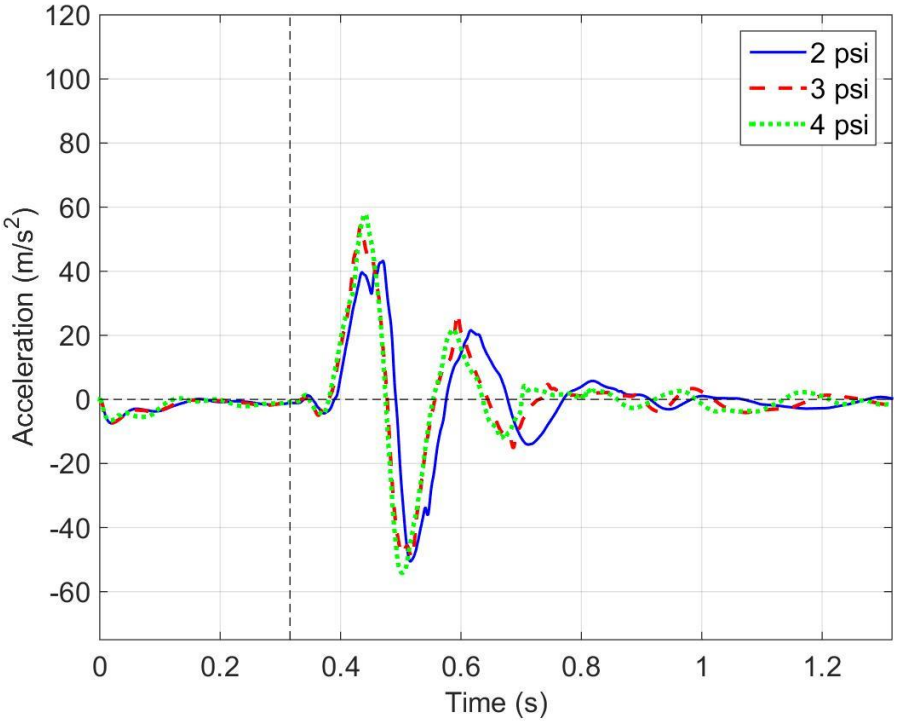

(a) 0.5 m drop hieght.

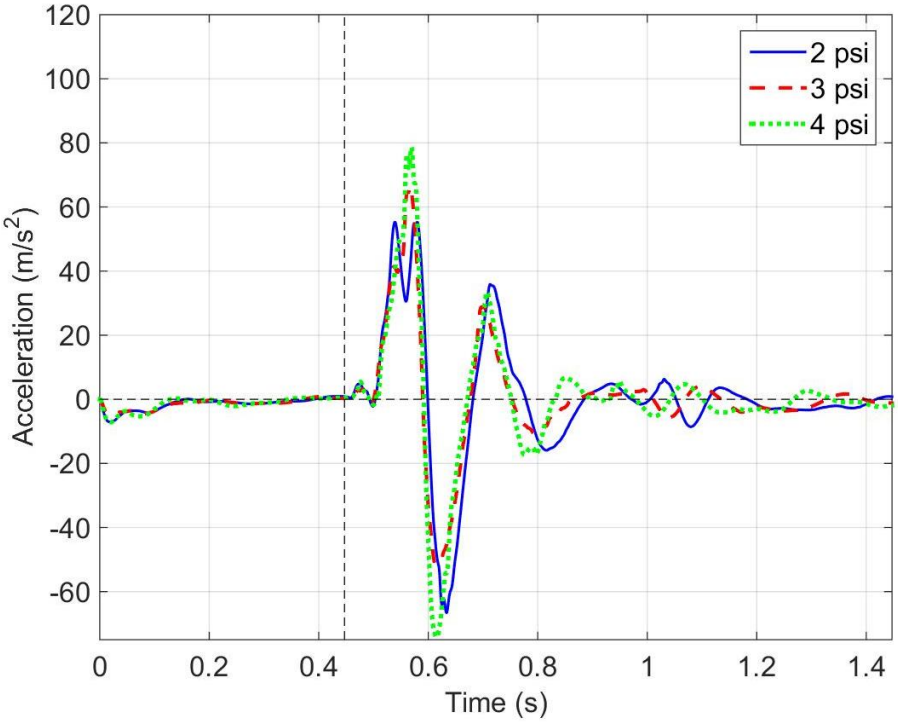

(b) 1 m drop hieght.

Figure 17: Mean acceleration-time history from the crew accelerometer (W_b weighted) during the full-scale drop tests with varied internal pressure of sponson and keel.

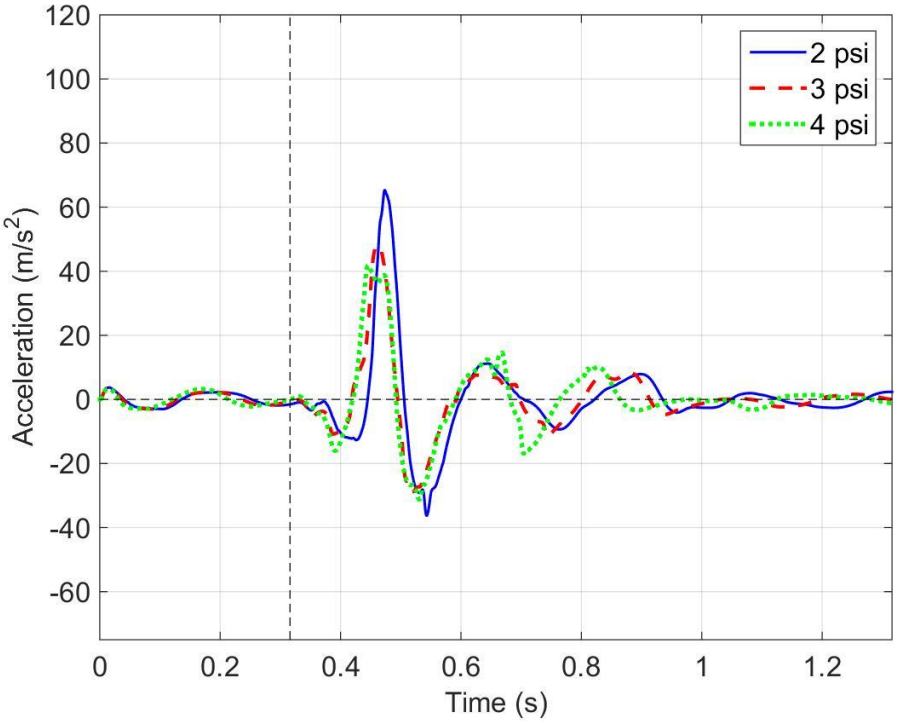

(a) 0.5 m drop hieght.

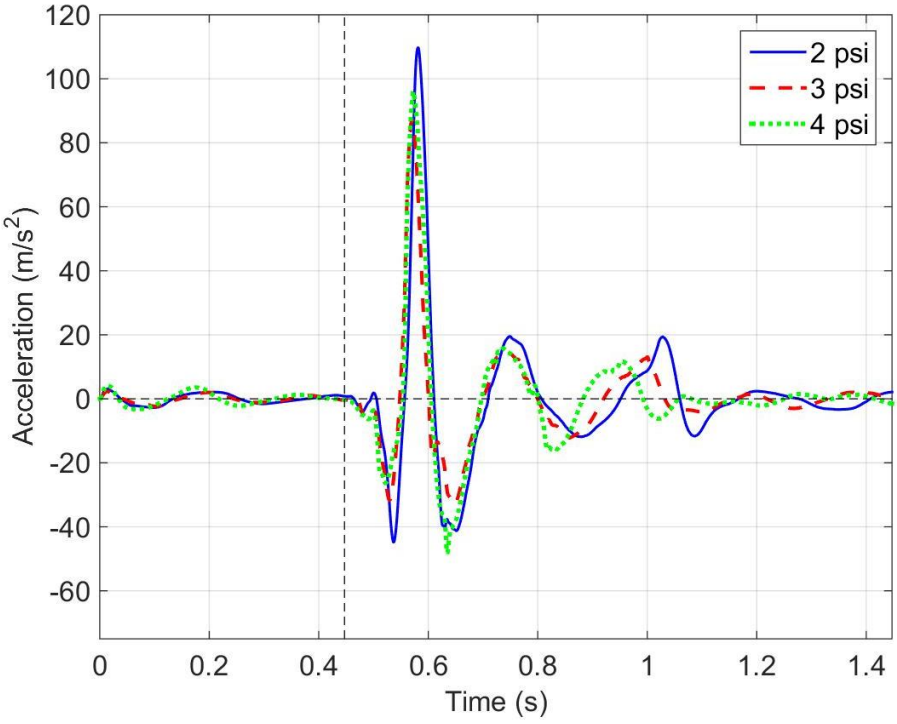

(b) 1 m drop hieght.

Figure 18: Mean acceleration-time history from the bow accelerometer (W_b weighted) during the full-scale drop tests with varied internal pressure of sponson and keel.

The peak duration was investigated because it was anticipated that the duration would vary inversely with the peak acceleration magnitude; however, no trends were found. Interestingly, Lee and Wilson (2010) (Figure 9) also found that there was minimal correlation between drop height and impact duration on the hydrodynamic impact of a racing sailboat; although, Lee et al. did find a strong relationship between drop height and peak pressure.

3.2.2 Error Analysis

It is inevitable that the full-scale drop tests would be less repeatable than the quasi-2D tests because the set up and environment were less controllable. The drop height was controlled by a crane and, although the crane was surprisingly accurate, the observable resolution of the drop height gauge was only ±10 mm. The water surface was not smooth because it was outside where the wind and tide generated small waves, regardless of settling time. The boat was suspended from a long cable (> 20 m) and the system acted as a pendulum, which also vary the drop height and caused an un-level roll and pitch angle. All of these variables were controlled and made repeatable through the drop height gauge by ensuring that the distance variation between the transom and water surface was less than ±10 mm. The drops were performed in a small marina so the surface waves generated during the slam did reflect off a nearby wall; however, the waves took 10 s to reflect and impact the boat. The impact took less than two seconds so the reflected waves did not affect the results.

4 Discussion

4.1 The Effect of Hydroelasticity on Whole Body Vibration

4.1.1 Quasi-2D drop tests

The effect of hydroelasticity on WBV has been quantified using two parameters: peak acceleration and VDV. The crest factors of all the drop tests (full and model scale) were above eight so VDV has been used instead of RMS. The peak acceleration and VDV from quasi-2D drop tests are shown Figure 19 and the error bars show two standard deviations. Peak acceleration and VDV consistently followed the same trends under all test conditions, which provides confidence in the WBV quantification parameters. The structural stiffness did effect peak acceleration and VDV and, importantly, peak acceleration and VDV were consistently higher for the MDF hull than the fabric hulls at all deadrise angles and drop heights. At 5° deadrise angle and 0.5 m drop height, peak acceleration and VDV increased as the hull stiffness increased; however, the trend in the fabric hulls changed at 1 m drop height. Nonetheless, peak acceleration and VDV were 13.8% and 13.2% (respectively) higher in the

MDF hull than the fabric hull with 1000 N/m pre-tension stress at 1 m drop height. At 0.5 m drop height, peak acceleration and VDV were 17.5% and 18.5% (respectively) higher in the MDF hull than the fabric hull with 0 N/m pre-tension stress. On the other hand at 15° deadrise angle, the structural stiffness appeared to have less effect on either peak acceleration or VDV, particularly with a 1 m drop height. Peak acceleration and VDV were 2.2% and 1.1% (respectively) higher in the MDF hull than the fabric hull with 0 N/m pre-tension stress at 1 m drop height. At 0.5 m drop height, peak acceleration and VDV were 9.3% and 10.6% (respectively) higher in the MDF hull than the fabric hull with 0 N/m pre-tension stress.

The measured differences could be due to experimental uncertainties and not statistical differences due to the hull stiffness; therefore, the null hypothesis was assumed. The null hypothesis was tested using a two tailed Student T-test and the results are shown in Table 2. The Student T-test results show that at 5° deadrise angle there were important statistical differences due the hull stiffness. The peak acceleration and VDV of fabric hulls and MDF hull were always significantly different with an average of 96.6% certainty (range from 87.2% to 99.2%) at 5° deadrise angle. Similarly, at 15° deadrise angle and 0.5 m drop height, the peak accelerations of the fabric and MDF hulls were always statistically different with a lowest certainty of 98.1%; however, at 15° deadrise angle and 1 m drop height there is minimal statistical difference, which agrees with observations.

The magnitude and statistical differences between the MDF hull and fabric hulls implies that hydroelasticity has a greater impact when the deadrise angle is low because there is larger magnitude and statistical differences at 5° deadrise angle than 15° deadrise angle. This agrees with the work of Faltinsen (1999) and Bereznitski (2001) where the importance of hydroelasticity increases by decreasing the deadrise angle; however, Faltinsen and Bereznitski also showed the importance of hydroelasticity increases by increasing the impact velocity. The impact velocity (or drop height) did not increase the percentage or statistical difference here.

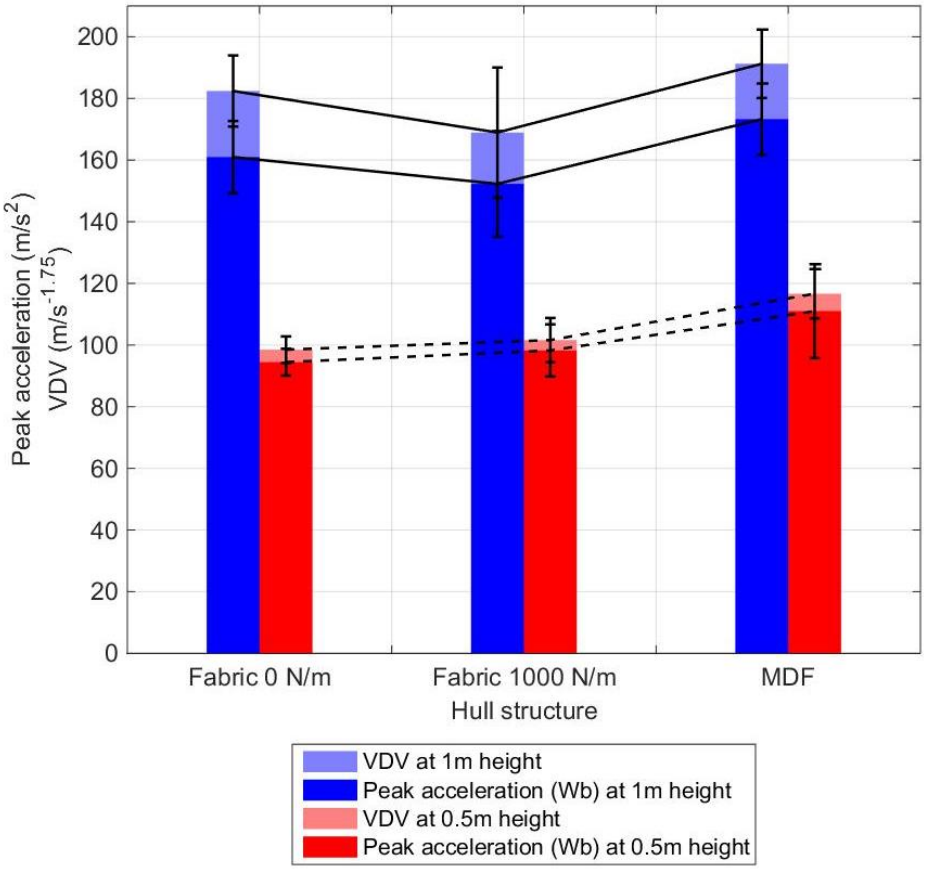

(a) 5° deadrise angle.

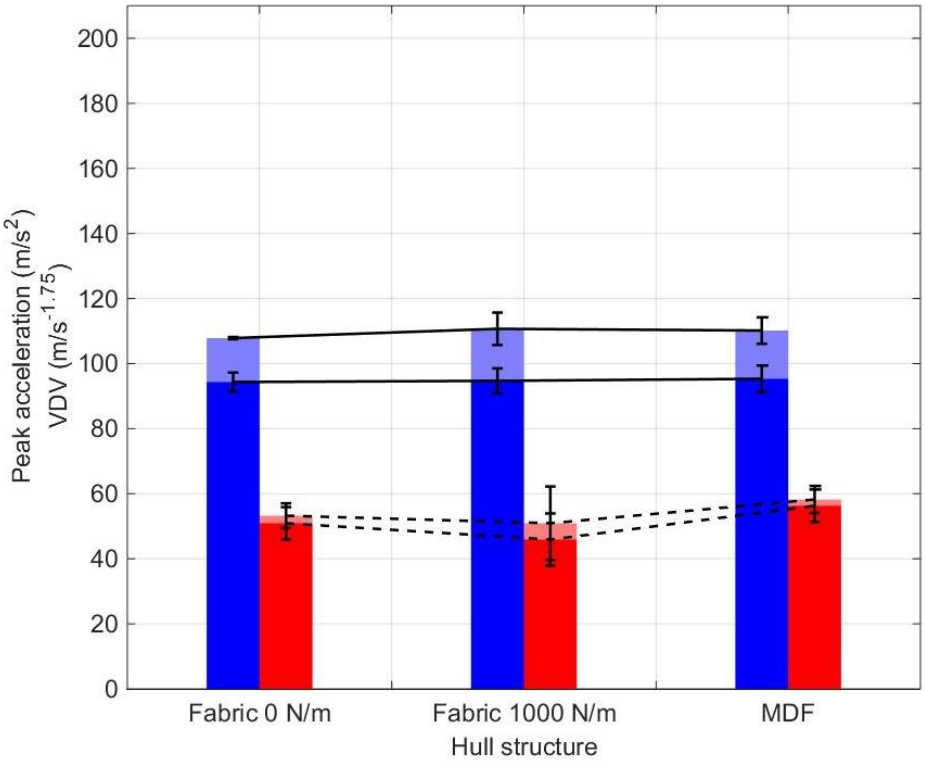

(b) 15° deadrise angle.

Figure 19: Quantification of WBV during the quasi-2D drop tests.

Table 2: Percentage statistical difference of peak accelerations and VDV from the 2D drop tests using a Student T-test; $\% = (1 - P_{value}) \times 100$; (bold text highlights % > 95).

Setup	Comparison	Peak acceleration (W_b weighted)	VDV
5° deadrise angle, 0.5 m drop height	0 N/m to MDF	93.5	**98.9**
	0 to 1000 N/m	65.9	63.5
	1000 N/m to MDF	93.6	**99.2**
5° deadrise angle, 1 m drop height	0 N/m to MDF	93.9	87.2
	0 to 1000 N/m	77.9	87.6
	1000 N/m to MDF	**97.5**	**96.8**
15° deadrise angle, 0.5 m drop height	0 N/m to MDF	**98.1**	**99.0**
	0 to 1000 N/m	**90.8**	47.6
	1000 N/m to MDF	**100.0**	**98.6**
15° deadrise angle, 1 m drop height	0 N/m to MDF	46.9	87.9
	0 to 1000 N/m	19.4	88.1
	1000 N/m to MDF	28.1	21.0

4.1.2 Full-scale drop tests

The peak acceleration and VDV from the transom, crew and bow accelerometers of the full-scale drop tests are shown in Figure 20. The peak acceleration and VDV consistently followed the same trends under all test conditions and again provides confidence in the WBV quantification parameters. First, the transom accelerometer (Figure 20a) revealed that the internal pressures had minimal effect on peak acceleration or VDV; however, this was expected because the structure at the transom is considerably stiffer than further forward. The inflatable keel does not extend up to the transom, which removes the effect of the keel pressure. The vertical transom panel will dramatically reduce sponson rotation and this should reduce the effect of the sponson pressure. Peak acceleration and VDV increased by 5.0% and 5.5% (respectively) as the internal pressure increased from 2 psi to 4 psi at 0.5 m drop height. At 1 m drop height, peak acceleration and VDV increased by 5.2% and 4.1% (respectively) as the internal pressure increased from 2 psi to 3 psi. The null hypothesis was assumed and tested with a two tail Student's T-test, see Table 3. The Student T-test results showed that there were some statistical differences, particularly between 2 psi and 4 psi at 0.5 m drop height. This suggests that the sponson pressure had a small effect on WBV but not significant compared to further forward longitudinally.

In the crew position (Figure 20b), peak acceleration and VDV did increase as the internal pressure increased. Peak acceleration increased by 17.2% and 31.8% as the internal pressure increased from 2 psi to 4 psi at 0.5 m and 1 m drop height, respectively; VDV increased by 9.1% and 14.3%, respectively. The Student's T-test (see Table 3) confirms that there were a statistical differences between 2 psi and 3-or-4 psi internal pressure with an average of 98.8% certainty (range from 94.6% to 99.9%). However, the negative peak acceleration in the crew position was larger than the positive peak acceleration caused by amplification of the W_b frequency weighting. The negative peak acceleration, shown in Figure 20c, did not follow the same trend as positive peaks; instead 3 psi internal pressure experienced the highest negative peak acceleration. The Student T-test results of the negative peak acceleration from the crew accelerometer are shown in Table 4. Nonetheless, VDV did decrease as internal pressure decreased, which accounts for positive and negative accelerations.

The peak acceleration and VDV measured by the bow accelerometer (Figure 20d) decreased as internal pressure increased; opposite to the crew accelerometer. Peak acceleration decreased by 63.4% and 18.4% as the internal pressure increased from 2 psi to 4 psi at 0.5 m and 1 m drop height, respectively; VDV decreased by 15.1% and 40.0%, respectively. The Student T-test (Table 3) showed that there were statistical differences at 0.5 m drop height with a mean certainty of 97.6% (range from 93.9% to 100.0%). At both drop heights, the null hypothesis was false between 2 psi and 4 psi internal pressure with a mean certainty of 97.1% (range from 90.3% to 100.0%).

The full-scale drop tests have shown that peak acceleration and VDV measured by the transom and crew accelerometers were reduced by decreasing the internal pressures; this indicates that WBV experienced at the transom and crew positions has being reduced by decreasing structural stiffness. In contrast, peak acceleration and VDV increased at the bow, which suggested WBV experienced at the bow increased; however, the crew of the D-class are position aft-wards and are not exposed to these accelerations. Nonetheless, this proves that internal pressures can change the human exposure to vibration during full-scale drop tests.

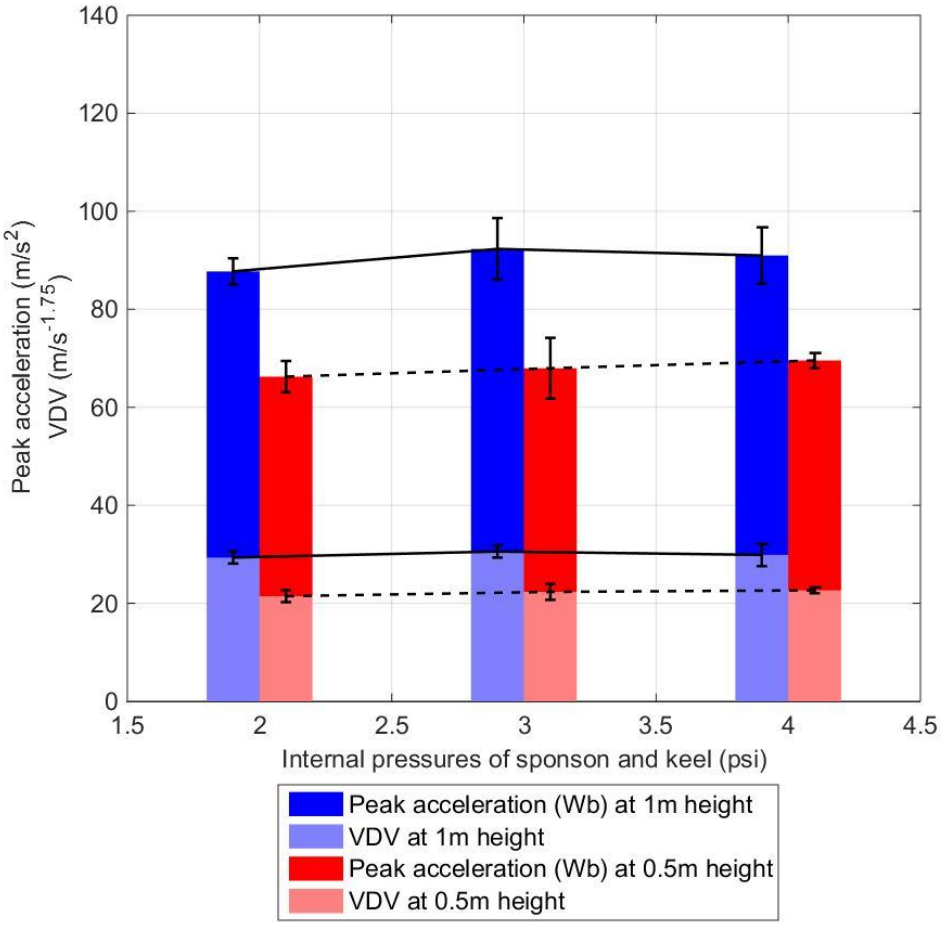

(a) Transom.

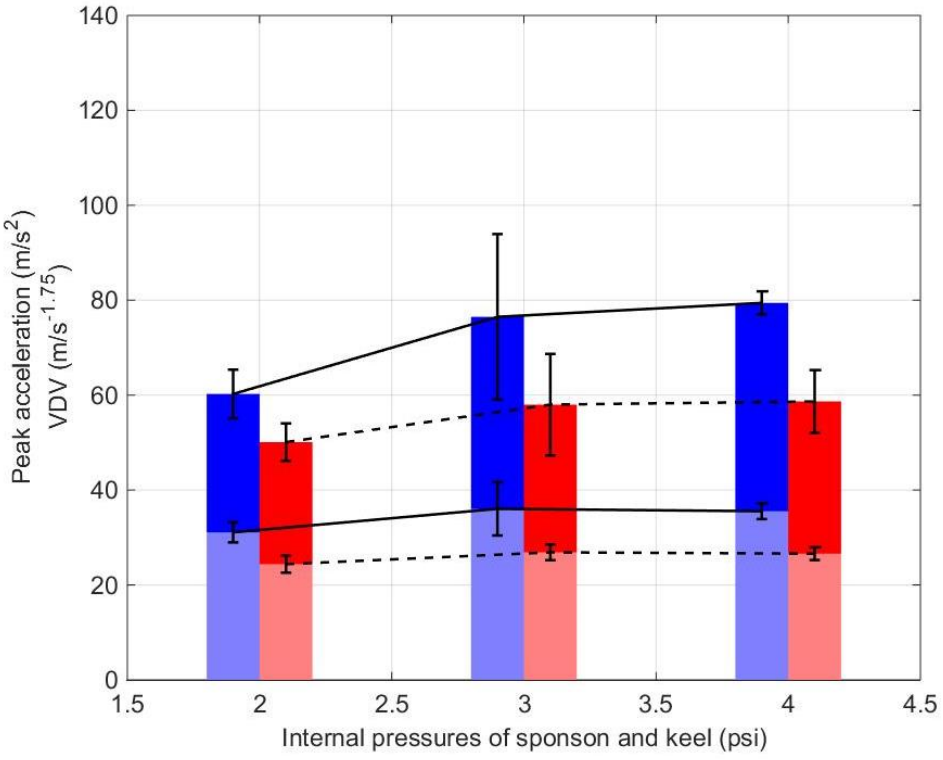

(b) Crew.

Figure 20: Quantification of WBV during the full-scale drop tests.

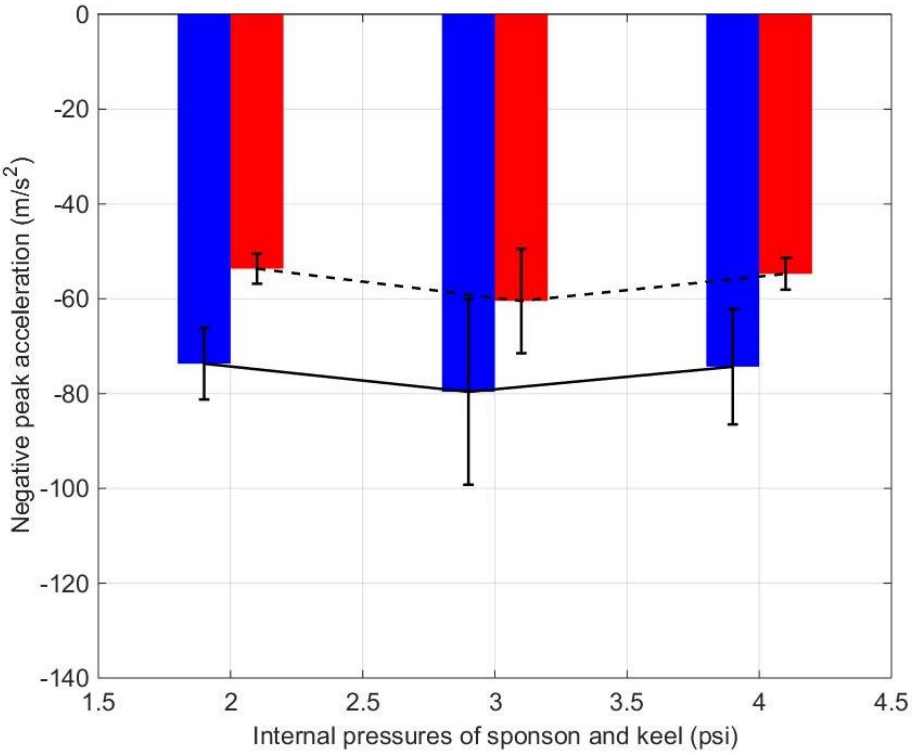

(c) Crew (negative peak acceleration only).

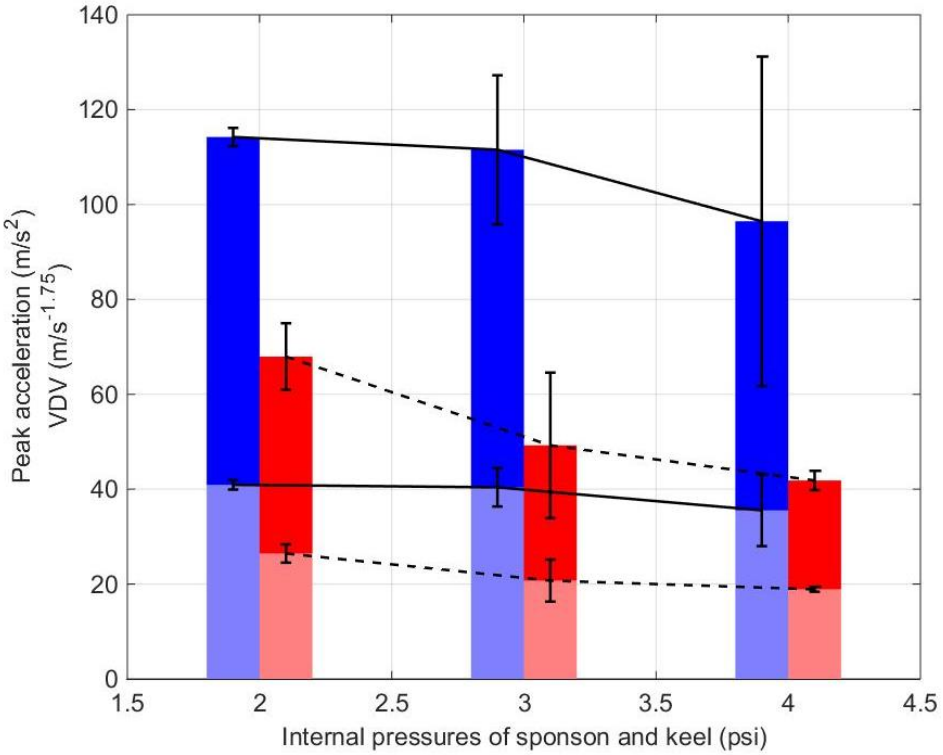

(d) Bow.

Figure 20(continued): Quantification of WBV during the full-scale drop tests.

Table 3: Percentage statistical difference of peak accelerations and VDV from the full-scale drop tests using a Student T-test; $\% = (1 - P_{value}) \times 100$; (bold text highlights % > 95).

Accelerometer Location	Drop height	Comparison	Peak acceleration (W_b weighted)	VDV
Transom	0.5 m	2 to 4 psi	**99.7**	**99.6**
		2 to 3 psi	71.2	90.2
		3 to 4 psi	70.5	60.5
	1 m	2 to 4 psi	92.1	67.0
		2 to 3 psi	**98.5**	**99.0**
		3 to 4 psi	38.3	64.4
Crew	0.5 m	2 to 4 psi	**99.9**	**99.8**
		2 to 3 psi	**98.9**	**99.9**
		3 to 4 psi	18.7	20.6
	1 m	2 to 4 psi	**94.6**	**98.4**
		2 to 3 psi	**99.7**	**99.6**
		3 to 4 psi	63.3	70.9
Bow	0.5 m	2 to 4 psi	**100.0**	**100.0**
		2 to 3 psi	**99.9**	**100.0**
		3 to 4 psi	93.9	91.8
	1 m	2 to 4 psi	90.3	**98.2**
		2 to 3 psi	52.8	45.0
		3 to 4 psi	77.5	93.8

Table 4: Percentage statistical difference of negative peak accelerations from the full-scale drop tests using a Student T-test; $\% = (1 - P_{value}) \times 100$; (bold text highlights % > 95).

Accelerometer Location	Drop height	Comparison	Peak acceleration (W_b weighted)
Crew	0.5 m	2 to 4 psi	59.0
		2 to 3 psi	71.1
		3 to 4 psi	**95.6**
	1 m	2 to 4 psi	**98.7**
		2 to 3 psi	**99.0**
		3 to 4 psi	90.2

4.2 A Hydroelastic Planing Craft?

Can structural stiffness be utilised to design a functional hydroelastic planing craft with the ability to reduce WBV? The first step to designing a hydroelastic planing craft is to find the root cause of the reduced WBV. The quasi-2D drop tests showed that panel deflection can reduce WBV and it is hypothesised that increasing panel deflection increases the damping within the system and absorbs more energy; therefore, reducing the energy outputted to the

crew. The root cause to the full-scale drop tests is far more complex. The contrast between the trends at the transom and crew accelerometer, and bow accelerometer could be explain by two hypotheses. First, the increased internal pressure of the keel increased the deadrise angle and structural stiffness at the bow causing better shock attenuation; however, the crew position should follow a similar trend if this hypothesis was true, which did not occur. Second, the decreased internal pressures allowed better transfer of vibrations within the dynamic response frequency range of human body from the transom to the bow via whipping that were; therefore, decreasing aft-ward accelerations but increasing the forward accelerations. If the root cause is found then it is possible to optimise the hull design and provide an overall reduction in WBV.

The quasi-2D drop tests provide an insight into the effect of deadrise angle on this hydroelastic interaction. The reduction in peak acceleration and VDV due to decreased structural stiffness was greater at 5° deadrise angle than 15°. The mean reductions (of both drop heights) between the MDF hull and fabric hulls in peak acceleration and VDV at 5° deadrise angle were 15.6% and 15.9%, respectively; however, at 15° deadrise angle, the mean reduction was only 5.8% and 5.9%, respectively. This suggests that a hydroelastic hull would be more suitable for HSC with shallow deadrise angles, like the D-class, or that the structural stiffness should be varied along the length of the vessel with the deadrise angle for an optimal solution.

So far hydroelastic slamming has the potential to provide an overall reduction in WBV; however, now compare it to the other solutions available to reduce the WBV on planing craft and the effect hydroelasticity may have on a planing craft. Forward speed is very important for planing craft and experienced helmsmen of the D-class report that the keel pressure will affect the forward speed; therefore, a hydroelastic hull will affect the forward speed. Dand et al. (2008) reported that a flexible planing surface can cause a phenomenon similar to porpoising on flat water but was removed by increasing the shear modulus of the hull fabric. Hydroelastic planing surfaces were also discussed by Halswell et al. (2012). On the other hand, these craft are used in heavy seas where the limiting factor to forward speed in waves is actually the WBV experienced by the helm and crew because they cannot cope with the slamming accelerations. So hydroelasticity may reduce flat water speed but the helm may sustain a higher forward speed in waves.

One major disadvantage for suspension seats and suspension decks is the increased weight of the craft but a flexible hull does not increase the weight. In fact, the US navy have developed a craft where a composite hull was treated as a membrane surface and this allowed

them to decrease the overall weight of the hull by 20%, see Wood (2011). It was stated earlier that the density of the D-class fabric was 57% lower than aluminium but the ultimate tensile strength was only 27% lower which also demonstrates that membrane structures could be lighter. Although, the reaction forces on the structure of a flexible craft may be considerably higher than a rigid craft. To counter act this, the structure will have to be redesigned and inevitably lead to a more complex and heavier structural design. This would increase the weight of the scantlings but the US navy still managed an overall weight reduction.

A major advantage for a hydroelastic hull is its simplicity; nothing has to be added to the craft to incorporate it. Suspension seats have to be added to the craft which restricts crew movement and raises the vertical centre of gravity, see Townsend et al. (2012). Suspension decks require a highly complex system of springs and dampers, see Coe et al. (2013). Fins, interceptors and trim tabs have to be added to the craft which will affect the hydrodynamics performance, increase fit out complexity and increase weight.

Table 5: Summary of the advantage and disadvantages of a hydroelastic slamming approach to reducing WBV.

Advantages	**Disadvantages**
• Reduced WBV aft-wards (in crew locations).	• Increased WBV forward (but crew do not experience this).
• Increased speed in waves.	• Reduced flat water speed.
• Reduction in weight.	• Complex structural design.
• Simplicity.	• Increase in cost.
• No change to operational ability.	

Hydroelastic slamming cannot solve the problem of WBV in planing craft on its own with the current level of knowledge but it does show promise for being part of a combined approach to reducing the WBV. If hydroelastic slamming can reduce the WBV and the overall weight, then the weight saving can be used to incorporate other WBV reduction strategies. This could lead to a significant overall reduction in WBV.

6. Conclusion

The effect of hydroelasticity slamming on the peak acceleration and VDV has been experimentally studied using quasi-2D and full-scale drop tests. The quasi-2D drop tests of a high-speed planing hull with hard chines varied the hull stiffness, deadrise angle and drop height. The full-scale drop tests of a RNLI D-class inflatable lifeboat varied the internal

pressures of the sponson and keel (which in turn varied the structural stiffness), and the drop height. The variation of acceleration along the length of the D-class was studied. The following conclusions were drawn:

- Hydroelasticity effected of the peak acceleration and VDV measured during quasi-2D and full-scale drop tests.
- Quasi-2D drop tests showed that WBV generated by a wooden hull were higher than the fabric hulls.
- Quasi-2D drop tests showed that hydroelasticity had a greater effect at low deadrise angle.
- Full-scale drop tests showed that increasing internal pressure of the sponson and keel of the D-class from 2 psi to 4 psi:
    - had minimal effect at the transom where internal pressure have minimal effect on structural stiffness; although, a reduction in WBV was measured.
        - 5.2% mean[3] increase in peak acceleration.
        - 4.8% mean[3] increase in VDV.
    - reduced the WBV experienced by the crew.
        - 24.5% mean[3] increase in peak acceleration.
        - 11.7% mean[3] increase in VDV.
    - increased the WBV experience at the bow; however, the crew are not exposed to these vibrations.
        - 40.9% mean[3] decrease in peak acceleration.
        - 27.6% mean[3] decrease in VDV.

There are still many unanswered questions about the effect of hydroelasticity on slamming and WBV that require further work. Nonetheless, this paper and corresponding work have shown the potential use of hydroelasticity to reduce the human exposure to vibration on high-speed planing craft. Membrane structures have been shown by Wood (2011) to reduce the overall weight of a craft whilst this work shows the potential to reduce the human exposure to vibration; therefore, a hydroelastic hull could be combined with other WBV reduction strategies to alleviate the risk of injury to the on-board crew, provide a better working environment and increase the crew's effectiveness during and after transit.

Further work should include examining the root cause to the change in WBV, possibly achieved through a systematic study with smaller variation increments of the test

[3] Mean of both drop heights.

parameters (stiffness conditions, drop heights and deadrise angles). A corresponding numerical model could be developed linked Wagner's theory with a membrane deformation model. Eventually, wave trials should be performed at model or full scale in regular and irregular waves. Allen (2013) showed that increased flexibility in hull panels lead to increased total force so structural loading of a hydroelastic planing craft also requires further work.

Acknowledgement

This work is supported by the RNLI and EPSRC, and a special thanks to the employee at ILC for their support during the full-scale tests.

References

Allen, D. P., Taunton, D. J., and Allen, R. (2008). A study of shock impacts and vibration dose values onboard high- speed marine craft. *International Journal of Maritime Engineering*, 150(A3):1-14.

Allen, T. D. (2013). *Mechanics of flexible composite hull panels subjected to water impacts.* PhD Thesis, the University of Auckland, URL: http://hdl.handle.net/2292/21184.

Bereznitski, A. (2001). Slamming: the role of hydroelasticity. *International Shipbuilding Progress*, 4(48):333-351.

Coats, T., Gowing, S., and Shen, Y. (2009). Porous hulls research - phase 1. *Technical report, Naval Surface Warfare Center*, Virginia, USA.

Coats, T., Haupt, K., and Lewis, J. (2003). Shock mitigation for personnel onboard high-speed combatant craft. *In Human Systems Integration Symposium*, VA.

Coe, T. E., Rutherford, K. T., Dyne, S., and Hirst, J. (2013). Technical solutions for shock mitigation on high speed government craft. *In SURV 8 - Surveillance, Search and Rescue Craft*, pages 1-12, Poole, UK.

Coe, T. E., Xing, J. T., Shenoi, R. A., and Taunton, D. J. (2009). A simplified 3-D human body - seat interaction model and its applications to the vibration isolation design of high-speed marine craft. *Ocean Engineering*, 36(9-10):732-746.

Cripps, R. M., Cain, C. F., Phillips, H. J., Rees, S. J., and Richards, D. (2004). Development of a new crew seat for all weather lifeboats. *In SURV 6 - Surveillance, Pilot and Rescue Craft*, RINA, pages 69-76.

Dand, I. (2004). RNLI D-class model: seakeeping measurements in head seas. *Technical Report C3356.06*, BMT SeaTech Limited.

Dand, I., Austen, S., and Barnes, J. (2008). The speed of fast inflatable lifeboats. *International Journal of Small Craft Technology*, 150(B2):23-32.

Ensign, W., Hodgdon, J. A., Prusaczyk, W. K., Shapiro, D., and Lipton, M. (2000). A survey of self- reported injuries among special boat operators. *Technical report*, Naval Health Research Centre, San Diego, UK.

Faltinsen, O. M. (1999). Water entry of a wedge by hydroelastic orthotropic plate theory. *Journal of Ship Research*, 43(3):180-193.

Faltinsen, O. M., Landrini, M., and Greco, M. (2004). Slamming in marine applications. Journal of Engineering Mathematics, 48(3/4):187-217.

Haiping, H. E., Bretl, J. P. E., VanSumeren, H., Savander, B., and Troesch, A. W. (2005). Model tests of a typical rib in waves. *Private communication*.

Halswell, P. K., Wilson, P. A., Taunton, D. J., and Austen, S. (2012). Hydroelastic inflatable boats: Relevant literature and new design considerations. *International Journal of Small Craft Technology*, 154(Part B1):39-50.

Hot RIBS (2015). http://hotribs.com/02articles/059-tube-materials/inflatable-boat-tube-materials.asp; last accessed on 15/11/2015.

Kapsenberg, G. K. (2011). Slamming of ships: where are we now? *Philosophical Transactions of the Royal Society A: Mathematical, Physical and Engineering Sciences*, 369(1947):2892_2919.

Lee, J. and Wilson, W. A. (2010). Experimental study of the hydro-impact of slamming in a modern racing sailboat. *Journals of Sailboat Technology*, SNAME, 1:1-29.

Lewis, S. G., Hudson, D. a., Turnock, S. R., and Taunton, D. J. (2010). Impact of a free-falling wedge with water: Synchronized visualization, pressure and acceleration measurements. *Fluid Dynamics Research*, 42(3):035509.

Lewis, W. J. (2003). *Tension structures: Form and behaviour*. Thomas Telford.

Lloyd, A. R. J. M. (1998). *Seakeeping: Ship behaviour in rough weather*. Ellis Horwood, 1st edition.

Maier-Schneider, D., Maibach, J., & Obermeier, E. (1995). A new analytical solution for the load-deflection of square membranes. *Journal of Microelectromechanical Systems*, 4(4), 238-241.

MCA (2007). The merchant shipping and fishing vessels: control of vibration at work regulations, 2007.

Myers, S. D., Dobbins, T. D., King, S., Hall, B., Ayling, R. M., Holmes, S. R., Gunston, T., and Dyson, R. (2011). Physiological consequences of military high-speed boat transits. *European Journal of Applied Physiology*, 111(9):2041-9.

Natzijl, P. W. (1998). Bringing a 1.0 metre buoyancy tube to sea on a 18.0 metre rigid hull. *In International Conference on Rigid Inflatables*, Weymouth, UK.

Ochi, M. (1964). Extreme behaviour of a ship in rough seas: slamming and shipping of green water. *Society of Naval Architects and Marine Engineers*.

Olausson, K. (2012). *Vibration mitigation for high speed craft.* PhD Thesis, Royal Institute of Technology, Stockholm, Sweden.

Pike, D. (2003). Inflatable tubes over advantages for small craft. *Ship and Boat International*, November (D):78-82.

Pond, C. (2005*). The control of vibration at work regulations*. Guidance on Regulations, Health and Safety Executive L140. ISBN 07176.

Rawson, K. J. and Tupper, E. C. (2001). *Basic Ship Theory: Volume 2.* Butterworth-Heinemann.

Riley, M., Coats, T., Haupt, K., & Jacobson, D. (2010, August). The characterization of individual wave slam acceleration responses for high speed craft. *Proceedings of the 29th American Towing Tank Conference* (pp. 21-30).

Schmidt, A. L., Paskoff, G., Shender, B. S., & Bass, C. R. (2012). Risk of Lumbar Spine Injury From Cyclic Compressive Loading. *Spine*, 37(26), E1614-E1621.

Townsend, N., Coe, T., Wilson, P., and Shenoi, R. (2012). High speed marine craft motion mitigation using flexible hull design. *Ocean Engineering*, 42:126_134.

Townsend, N. C., Wilson, P. A., and Austen, S. (2008a). Sea-keeping characteristics of a model RIB in head seas. *International Journals of Maritime Engineering*, 151.

Townsend, N. C., Wilson, P. A., and Austen, S. (2008b). What influences rigid inflatable boat motions? *Proceedings of the Institution of Mechanical Engineers, Part M: Journal of Engineering for the Maritime Environment*, 222(4):207-217.

Wood, K. (2011). Re-inventing the RHIB: Shock mitigation. *Composite World*, pages 1-4.